A burn-through model for textile membranes in buildings as a tool in performance based fire safety engineering

Joel Andersson
Andreas Lennqvist

Department of Fire Safety Engineering and Systems Safety
Lund University, Sweden

Report 5347, Lund 2010

The thesis was funded by the Technical Research Institute of Sweden

A burn-through model for textile membranes in buildings as a tool in performance based fire safety engineering

Joel Andersson
Andreas Lennqvist

Lund 2010

A burn-through model for textile membranes in buildings as a tool in performance based fire safety engineering

Joel Andersson & Andreas Lennqvist

Report 5347
ISSN: 1402-3504
ISRN: LUTVDG/TVBB-5347-SE

Number of pages: 91
Illustrations: Joel Andersson & Andreas Lennqvist

Keywords:
Computational Fluid Dynamics, Fire Dynamics Simulator, burn away option, pyrolysis models, textile membranes, complex geometries, uncertainty.

Sökord:
Fluiddynamik, Fire Dynamics Simulator, avbrinningsmodell, pyrolysmodeller, textila membran, komplexa geometrier, osäkerhet.

Abstract
Using the characteristics of a fire scenario as a starting point, the authors illuminated the risks using textile membranes as a building material. The burning away of the membrane and the opening of a natural smoke evacuation was chosen for further studies. Using input from validation experiments the authors simulated these experiments in FDS to explore the agreement. There was uncertainties in finding the correct input data, especially determining the heat of combustion and the width of the pyrolysis range. Results showed that it is possible to use the burn away option in FDS to model the opening up of a hole in textile membranes. However, using textile membrane as a fire safety precaution for natural smoke evacuation is not reasonable. Furthermore the report shows that it is possible to import complex geometries to FDS and use the burn away option as well. However, at the moment it is impossible to accurately simulate complex geometries for fire safety design purposes.

Brandteknik och Riskhantering
Lunds tekniska högskola
Lunds universitet
Box 118
221 00 Lund

brand@brand.lth.se
http://www.brand.lth.se

Telefon: 046 - 222 73 60
Telefax: 046 - 222 46 12

Department of Fire Safety Engineering
and Systems Safety
Lund University
P.O. Box 118
SE-221 00 Lund
Sweden

brand@brand.lth.se
http://www.brand.lth.se/english

Telephone: +46 46 222 73 60

Summary

The interest in the use of textile membranes as a building material has grown. They are already on the market and used in a wide range of buildings, such as sports arenas, exhibition halls and other common rooms. The use of membranes in large constructions gives the constructer a possibility to create new, creative and often complex forms in buildings. This use is new and understanding of how these materials behave in fire is inadequate. However research is underway in the area, including an inter European project called Contex-T "Textile Architecture – Textile Structures and Buildings of the Future", where the Technical Research Institute of Sweden (SP) is a party. This thesis is one of the tasks SP has shouldered in the project.

Using the characteristics of a fire scenario as a starting point, the authors have performed a literature study that illuminates the risks using textile membranes as a building material. From this study the burning away of the membrane and the opening of a natural smoke evacuation was chosen for further studies. SP has performed fire tests of polyvinyl chloride / polyester membranes in a ISO-room to examine their behaviour in fire and the burning away and hole opening in particular. The authors has then simulated these experiment and explored the agreement between them and the Computational Fluid Dynamics (CFD) code, Fire Dynamics Simulator (FDS).

There are uncertainties in finding the correct input data, especially determining the heat of combustion from the cone calorimeter tests and the width of the pyrolysis range from the thermo gravimetric analyser. When using a wide possible range of several parameters, where most are sensitive to change, it becomes more difficult to find the true input and successfully emulate the validation experiments.
Results show that it is possible to use the burn away option in FDS to model the opening up of a hole in textile membranes. However, no simulations has perfectly mimicked the validation experiments and in a lot of cases the difference has been extensive. Great precaution should be taken when using the burn away option for fire safety design purposes.

From the results of this study the conclusion can be drawn that an opening will not occur until the flame reaches the ceiling. When the hole reaches a size that will evacuate a considerable amount of smoke the conditions in the room are not acceptable for personnel evacuation. In other words: using textile membrane as a fire safety precaution for natural smoke evacuation is not reasonable.

Finally the report shows that it is possible to import complex geometries to FDS and use the burn away option as well. However the fact that only Cartesian coordinates are allowed in FDS is a huge problem. At the moment this makes it impossible to accurately simulate complex geometries for fire safety design purposes.

Sammanfattning

Intresset för att använda textila membran som byggnadsmaterial har ökat. Materialen finns redan på marknaden och används i en lång rad byggnader, såsom idrottsarenor, utställningshallar och andra samlingslokaler. Användning av dessa membran i stora konstruktioner ger konstruktören en möjlighet att skapa nya, kreativa och ofta komplexa former. Detta användningsområde är nytt och förståelse för hur membranen uppför sig i en brand är otillräcklig. Forskning pågår dock inom området, bland annat genom ett europeiskt projekt kallat Contex-T " Textile Architecture – Textile Structures and Buildings of the Future ", där Sveriges Teniska Forskningsinstitut (SP) är delaktig. Detta examensarbete utgör en del av det uppdrag SP har i projektet.

Genom att utgå från ett brandscenario och egenskaperna för detta har författarna gjort en litteraturstudie som belyser riskerna med att använda textila membran som byggnadsmaterial. Utifrån denna studie valdes membranets avbrinning samt hålbildning för att uppnå naturlig brandgasevakuering för vidare studier. SP har genomfört valideringsexperiment i ISO-rum uppbyggda av membran gjorda av polyvinylklorid och polyester för att undersöka deras beteende i brand och i synnerhet avbrinning och hålöppning. Författarna har simulerat dessa experiment med Fire Dynamics Simulator (FDS) för att utforska överensstämmelsen. FDS är en Computational Fluid Dynamics-kod (CFD).

Det finns osäkerheter i att hitta rätt indata, särskilt vid fastställandet av förbränningsvärmen från konkalorimetertester och pyrolysområdet (pyrolysis range) testat i instrumentet thermo gravimetric analyser. Med ett stort antal parametrar med osäkra värden, där de flesta är känsliga för förändring, blir det svårt att hitta riktiga ingångsvärden och framgångsrikt efterlikna valideringsexperimenten.

Resultaten visar att det är möjligt att använda burn away-optionen i FDS för att modellera öppnandet av ett hål i textila membran. Däremot har ingen simulering perfekt efterliknat valideringsexperimenten och i många fall har skillnaden varit betydande. Stor försiktighet bör iakttas vid användning av burn away-optionen för brandteknisk dimensionering.

Från resultaten av denna studie kan slutsatsen dras att ett hål inte kommer uppstå innan flamman når taket. När hålet når en storlek som evakuerar en stor mängd brandgaser är förhållandena i rummet inte acceptabla för personevakuering. Med andra ord: att använda naturlig brandgasevakuering som en brandteknisk säkerhetsåtgärd i byggnader av textila membran är inte rimligt.

Slutligen visar rapporten att det är möjligt att importera komplexa geometrier till FDS och använda burn away-optionen. Men det faktum att endast rätvinkliga koordinater är tillåtna i FDS är ett stort problem. Att simulera komplexa geometrier för brandteknisk dimensionering anses därför för tillfället orimligt.

Preface

The authors would like to thank the following persons for their help during the work on this thesis:

Berit Andersson

Patrick van Hees

Petra Andersson

Per Blomqvist

Karim Andersson

Pontus Enander

CONTENTS

1 Introduction

This report is a master thesis in risk management specialized in fire engineering and comprise 30 ECTS credit points (hp). It was written at the Department of Fire Safety Engineering and Systems Safety at Lund University in cooperation with the Technical Research Institute of Sweden (SP).

1.1 Background

The interest in the use of textile membranes on a large scale in stationary and mobile buildings has grown. The use of textile membranes in large constructions gives the constructer the possibility to create new, creative and often complex forms in buildings. Textile membranes are already on the market used in a wide range of buildings, such as sports arenas, exhibition halls and other common rooms. See Figure 1, Figure 2 and Figure 3 below. This use of textile membranes is new and understanding of how these materials behave in fire is inadequate. The use of the material introduces new risks, such as how the construction and fire characteristics impact evacuation and fire development. However, research is underway in the area, including an inter European project called Contex-T "Textile Architecture – Textile Structures and Buildings of the Future", where SP is included as one of over 30 (research) parties from ten countries. The project aims at investigating the advantages with light weight building of textile membranes and to study the materials considering light performance, architecture, economy and safety issues. (1)

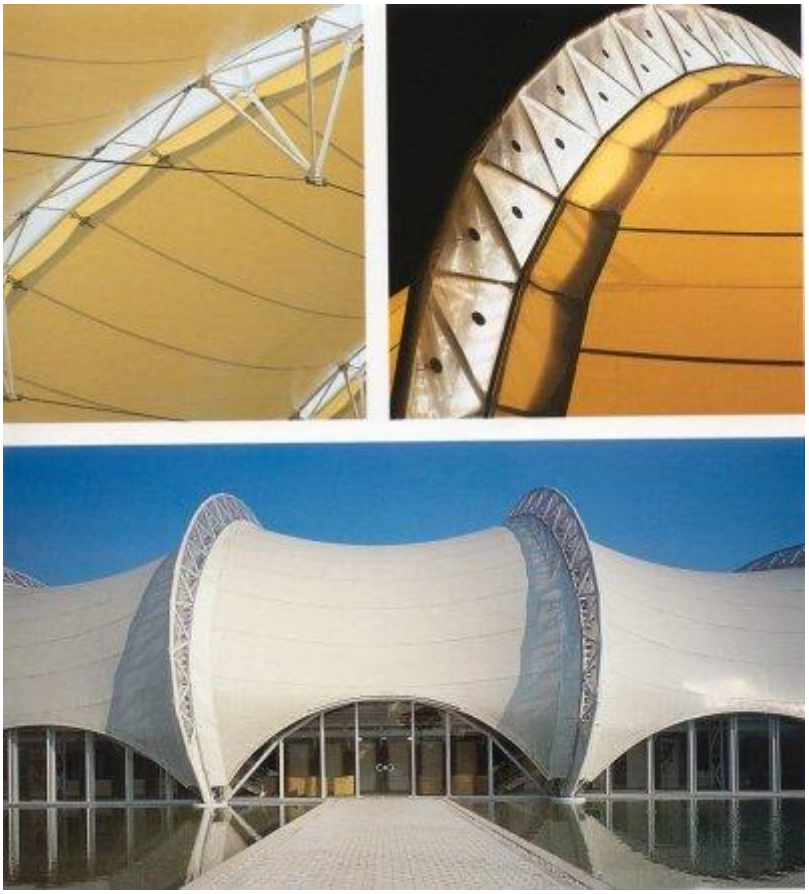

Figure 1. Centro M & G Ricerche, Venafro, Italia, 2900 m^2, PVC coated polyester, constructed in 1991. (2)

Figure 2. Centro M & G Ricerche, Venafro, Italia, PVC coated polyester, covered area 2 900 m², constructed in 1991. (3)

Figure 3. Zenith, a music palace able to contain 10 000 people, Strasbourg, France, silicone coated fibreglass, surface area: 12 000 m², constructed in 2007. (4)

Existing test methods for fire testing of materials are ill-fitted for textile membranes. Therefore more extensive testing and more unorthodox methods have been used. An expectation with the use of the textile membrane is that a natural smoke evacuation will occur when holes in the membranes are opened due to fire. This has not adequately been validated in real experiments. SP has therefore performed fire tests of various polyvinyl chloride (PVC)/polyester (PES) membranes in a so-called ISO-room to examine their behaviour in fire. The materials are built up of two kinds of polyester threads, one lengthways and one edgeways, coated in PVC. SP has also begun simulations with a computational fluid dynamics code (CFD) to examine whether the program adequately mimics the reality of, for instance, the burning away and hole opening of textile membrane. These simulations have in some cases shown good and in other cases bad consistence with the experiments. This

inconsistency is a problem that makes it impossible to use simulation software to carry out fire engineering dimensioning without carrying out large scale tests.

The authors' task is therefore to explore the degree of agreement between experiments and simulations to see if the program is reliable to use to simulate fires in buildings of textile membrane. It must also be considered whether CFD codes are suitable to simulate more complex geometries of textile membranes.

Related studies in this area have, among others, been performed by Tor Lindström and David Lund (5) and Leif Staffansson (6). Lindström and Lund illustrates how uncertainties in input variables can be handled with Monte Carlo simulations. Their results influence the authors' view of the uncertainties of the results in this thesis. Lindström and Lund's (5) results are further discussed in chapter 7.

The CFD program, Fire Dynamics Simulator (see further in chapter 5), enables the user to model flame spread. Staffansson (6) has evaluated the possibility to use this option to create a design fire. He has shown that the modelled flame spread is very dependent on the input parameters and the setup of the model. The uncertainties he observes has been important for the authors' understanding of the pyrolysis models used in this thesis. Staffansson's results are further discussed in chapter 7.

1.2 Objectives

The objective is to investigate whether Computational Fluid Dynamics (CFD) simulations can give a realistic picture of a fire in a building of textile membranes. The Fire Dynamics Simulator (FDS, see chapter 5) will be chosen as a tool for this purpose. The thesis also intends to investigate if FDS can accurately simulate fire in complex geometries of textile membranes. Together with a literature study the intention is to increase the understanding of the fire hazards with these new materials. Constructions with textile membranes and the materials fire properties are relatively untested.

The objectives are:

- Simulate and validate the experiments performed in ISO rooms to reach better agreement between simulations and experiments. Focus will be on studying hole openings and temperatures. To explore grid independence will be a part of the simulation work.
- Simulate a fire in a complex geometry.
- Illuminate the risks that are introduced by the use of textile membranes as a construction material.

1.3 Limitations

The following are the limitations of the report.

- Only one CFD code was used, namely FDS5. This tool introduces uncertainties, further discussed in chapter 7.
- Only two textile membranes were used.
- Only two experimental line-ups with each material were used.
- Only one run for each line-up.
- No real scale experiments.
- No experiments on complex geometries.

- Due to limited time and insufficient computer performance the simulations level of detail was limited, because the grids need to be adapted to the size of the geometry. See discussion in chapter 8.
- The authors' knowledge of FDS5 is only based on the course Simulation of Enclosure Fires V BR200, the FDS User Guide (7), discussions with SP, discussions with supervisors and observations from using the program. A lot of the conclusions are based on repeated simulations and not purely on theoretical knowledge of the program. This is partly due to the limited and often insufficient information on the burn away option in the FDS User Guide (7).

Some of the limitations have been made to limit the number of simulations and fit the project within the limits of the thesis.

2 Methodology

To provide answers to the objectives described in the previous chapter a risk identification with textile membranes, four room fire experiments and a large number of simulations have been performed.

2.1 Risk identification

The risk identification is mainly a literature study and is aimed at illuminating the risks using textile membranes as a building material and qualitatively discusses these risks. To accomplish this a fundamental understanding of the combustion process of plastics is necessary. Thus the chapter starts with a summary of relevant literature in this area. Using the characteristics of a fire scenario as a starting point, the risks with textile membranes are thereafter identified. These risks are loosely compared to the correlating risks with conventional building materials.

2.2 Experiments

The validation experiment described in chapter 1 was conducted by the Technical Research Institute of Sweden (SP) in Borås. The purpose of the experiments was to provide validation for the simulations. Photos, notes and extensive measurements of temperatures, visibility, smoke production and smoke velocities were recorded during the tests (1).

2.3 Simulations

The experiments described above were simulated in the computational fluid dynamics (CFD) software Fire Dynamics Simulator (FDS). The purpose was to explore the burning away of the membrane and thus the hole opening and see if the simulations were consistent with the experiments.

Finding relevant input parameters turned out to be tough. Different test methods such as the cone calorimeter, the thermo gravimetric analyser and the transient plane source, performed by SP, were used to determine some parameters. Others were found in specialist literature. The insecurity with input parameters led to a great number of simulations and divergence in the output.

3 Risk identification of textile membranes

Textile membranes are relatively new among building materials. All new materials should ideally go through extensive testing before being introduced on the market. When tests are not performed there is a danger that the user will believe that the new material will perform as a conventional well-known material. This chapter will therefore focus on clarifying the complex behaviour of burning plastics and an identification of the risks with textile membranes relative to classic building materials. The risk identification is purely qualitative and is made with a somewhat limited knowledge of the practical use of the materials since the main emphasis of the thesis is the simulations. However the risk identification gives the reader an idea on the possible hazards related to using these innovative materials. The risk identification is also limited to the type of textiles membranes which were used in the testing and in the project. It does not cover all type of possible textile membranes.

Some of the parameter values for the textile membranes used in this chapter and the entire thesis come from tests performed by SP and the manufacturer. The other values are taken from literature sources in which case the textile membranes have been assumed to equal PVC.

3.1 Burning of plastics

The textile membranes tested by SP and referenced to in this report are made up of a combination of polymers, namely polyvinyl chloride (PVC) and polyester (PES). Unfortunately specific details about the polymers from the manufacturers have been left out due to competition and replication. Since there are several types of PVC and polyester with different attributes and of these only a handful has been researched one has to generalize (8). Using polymers as a building material introduces new possibilities but also uncertainties and obstacles. This chapter will in short describe the combustion process of polymers, for the purpose to interpret and draw conclusions from the experiments and tests performed by SP. A basic knowledge of combustion of polymers is vital for identifying risks with this new building material.

Polymers are used for many purposes and are represented in many applications, due to its light-weight, high-performance and usually cost-effective properties. Like other organic compounds most polymers will combust in environments with enough oxygen. Because of the flammability of the polymers their range of appliance becomes limited. The problems becomes even greater with the toxic by-products which can be released when polymers combust. (9)

When heat is applied to a polymeric material both its physical and chemical properties change. Thermal degradation effects the physical, mechanical and/or electrical property of a polymer application whereas thermal decomposition change the chemical structure by breaking down the long polymer chains and produce combustible volatiles (10). The process of combustion of polymers is highly complex. Compared to flammable liquids for example where the gasification process is evaporation, which rate correlates to the equilibrium vapour pressure at the surface (10). However, polymers in their original state are involatile. Before combustion can occur the huge molecules has to be broken down so vaporization becomes possible (11). Since an assortment of different smaller molecules made up of different chemicals species forms during decomposition, some molecules will evaporate before others. This is due to the difference in equilibrium vapour pressure between molecules. When the concentration of volatile fuel gases reaches the

flammability limit ignition occurs. Because of the diffusivity of oxygen, the low solubility and the low oxidation rate at the decomposition temperature polymers will not burn in the condensed phase (12). When a plastic burns its surface temperature will not significantly go beyond the thermal decomposition temperature because all the excess energy from the flame will be used up for vaporization of new fuel gases instead of raising the temperature of the solid (12). This process will go on until all the volatile fuel is depleted.

The reasoning above leads to the conclusion that the decomposition temperature should be close to the surface temperature of plastics at ignition. (12). During flaming combustion it is the heat transfer which will determine the burning rate, heat release rate, and smoke production. This is due to the difference in reaction rates between the more rapid thermal decomposition and the heat absorption which occur at the surface of the plastic (12). However, thermal stability, fuel fraction, heat of combustion and products of combustion are determined by the chemical composition of the polymer.

Complete combustion of polymers is rare. Most leave residue behind in the form of either carbonaceous char, like PVC, or inorganic residue originating from heteroatoms (10). When carbonaceous char forms due to heat it usually involve a swelling effect on the surface of the material, thus increasing volume and decreasing density. This decreases the flammability greatly for a polymer. The char becomes a porous layer which considerably reduces the flow of heat from the gaseous combustion zone to the condensed phase beneath the char, thus slowing down the thermal decomposition process (12). However, if the char is carbonaceous all together it can always be burned by surface oxidation at higher temperatures. In contrast, inorganic residue can form a layer of glass like character which can create an impenetrable barrier for volatiles and ultimately cease the thermal decomposition (10). A combination of these residues is not unheard of. However, the production of char is not always a helpful fire retarding process. When char combusts in solid phase it might induce sustained smouldering combustion (12). As a result of enhancing a polymeric material with charring properties for fire retarding purposes you may just have reduced one risk but created another.

Another prospect of polymers is their physical changes during the influence of heat. Most polymeric materials have a considerably lower melting temperature compared to their ignition temperature, thus potentially creating larger combustible surfaces which yield a higher heat release rate among other things. However, thermoplastics in general demonstrate no substantial willingness to flow during heating or combustion (12). This is probably because of high viscosity or in some cases that apparent decomposition, which generates volatiles, occurs before melting i.e. the decomposition temperature is lower than the melting temperature. An exception of thermoplastics that flow readily are polyethylene plastics and polyester.

Yet another property of many plastics is their tendency to produce toxic by-products during combustion. Polyvinyl chloride for example generate hydrogen chloride gas when exposed to temperatures between 500-550 K (12). However, significant production does generally not start until temperatures above 600 K. This depends on which type of PVC that is combusting. More on combustion products in 3.2.7.

3.2 Risk identification

A knowingly taken risk is better than an unknowingly taken risk. Even if there may be problems quantifying the former, one knows nothing of the later. See corresponding discussion on uncertainties and errors in chapter 7. To make visible the great differences between textile membranes and conventional building materials this chapter includes a risk identification and a short qualitative analysis of these risks. Textile membranes will be compared to the most common building materials, such as concrete, wood, brick, plaster (board) and steel. Focus will be on emergency evacuation and therefore the early stages of the fire scenario when escape from the building is still possible. Figure 4 below shows parameters that influences the fire scenario.

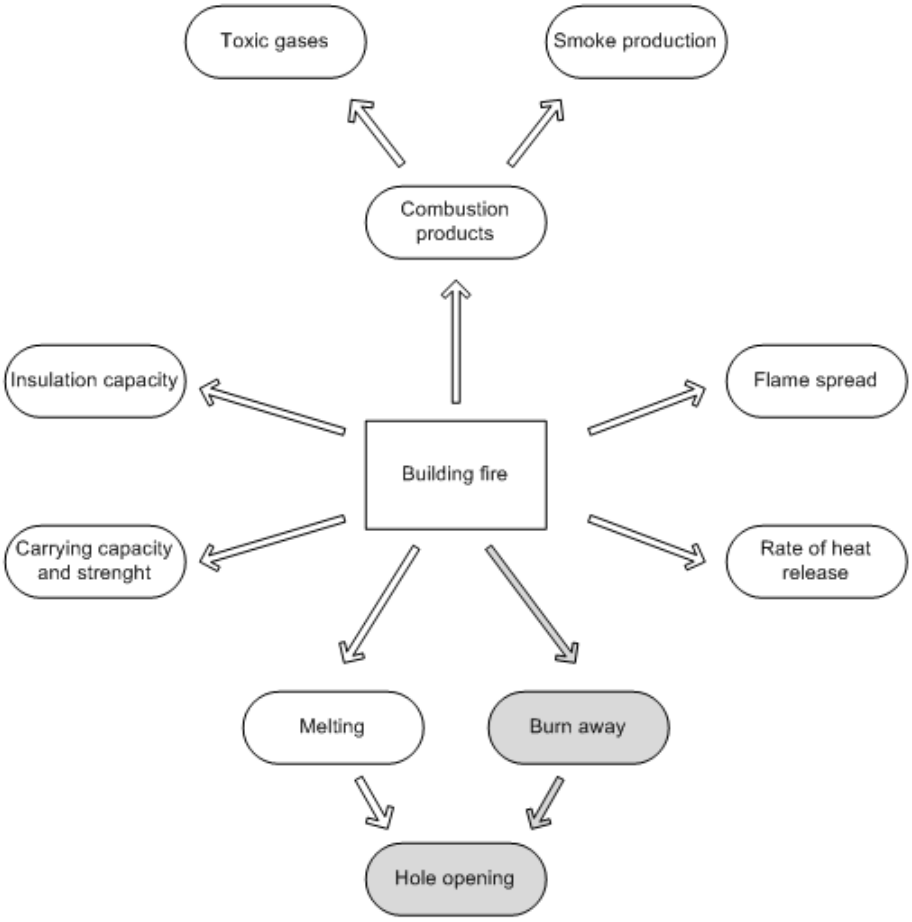

Figure 4. Characteristics of a fire scenario. The process of identifying the risks uses this mind map as a foundation. The characteristics marked grey are the core of the thesis and the only characteristics examined in detail beyond this chapter.

Some of the parameters depend highly on the surface layers while others depend on the load-bearing building materials. Buildings of textile membranes are typically constructed of a structure with steel beams and cables holding up large sheets of textile membranes. A great difference between buildings of conventional materials and buildings of textile membrane is that the conventional ones have layers of materials where some withstand the elements, some are load-bearing, some insulating and some possess the desired surface attributes whereas the textile membrane often has to account for all but the load-bearing parts of a building.

3.2.1 Heat release rate

The size of the fire is a very important parameter. This parameter has much to do with the amount of combustible material in the room. The rate of heat release has a very direct impact on the fire scenario if the surface material does not withstand the heat.

3.2.2 Flame spread

Textile membranes burn and if the rate of heat release is great enough the flames will spread. The flame spread will, as with all materials, be greatest upwards. Horizontal flame spread and flame spread downwards takes more time. (13) Buildings of textile membranes does in many ways not live up to Boverket's Building Regulations (BBR) concerning fire properties. A place of assembly should for example have surface materials of at least Class B (14). Preliminary tests does suggest that one of the two membranes used in this thesis (B8103) only reaches Class E (15) when testing its surface layer properties. When the criteria in BBR are not met it has to be demonstrated with so called analytical design that the total fire protection of the building will not be lowered by the lapses in choice of materials or design (16). There are however a textile membrane in the Contex-T project that lives up to the demands of Euroclass B (17). That material was introduced in the project too late to be included in this thesis. The conventional materials all have a higher Euroclass than E. Unprotected wood panelling is for example given a D in the same kind of testing (18).

The experiments have shown that the tested membranes need an almost direct contact with the flames to sustain flame spread. This is of course not true for all textile membranes. But the kinds of buildings that are built with these materials tend to be airy, contain low amounts of material and poorly insulated. These attributes lessens thermal build-up which is vital for flame spread. In other words: textile membranes does not generally show good qualities when it comes to flame spread, but the buildings they are used in does.

Falling down of the membrane during a fire will probably not contribute to the fire in a significant way since the material is very thin and the fire probably has to be considerable to cause this sort of fall down. But the material might well contribute to the flame spread and worsen the situation for evacuating persons. Hot polyester will flow readily as described under 3.1 above.

3.2.3 Burn away, hole opening

Not many conventional buildings will burn away to the extent that a hole will open. At least not under the evacuation part of the fire scenario. As seen in the experiments, the textile membrane closest to the flame will burn away and a natural smoke evacuation will open up. This lets part of the smoke layer out, lowers the temperature and will possibly improve the conditions for personnel evacuation. This feature gives the textile membranes an advantage on conventional building materials if, but only if, the hole opens up when personnel evacuation is still possible.

3.2.4 Melting, hole opening

Melting may lead to flame spread as mentioned under 3.2.2 but also hole opening. To prevent spread of fire inside a fire compartment melting or dripping outside the fires immediate proximity is not allowed in the BRR (19). None of the mentioned conventional materials will melt during the early stages of the fire scenario.

3.2.5 Carrying capacity and strength

It is essential for a safe evacuation of a building that it will withstand a fire during the evacuation time without collapsing. Some buildings of textile membranes are held up by concrete parts such as staircases and some buildings of lesser size are held up by inflating air into tubes of the textile. The most common way though is to hold up sheets of membrane with beams and wires of steel. The weak part of such a construction is probably the textile membrane itself. It has a much lower melting temperature than steel (20) and will not be able to carry its own weight when exposed to high temperatures. In such a scenario whole slabs of burning or melting membrane might fall down, obstruct evacuation, alter the tensions in the structure and maybe lead to greater collapse.

3.2.6 Insulation capacity

A well insulated building keeps the heat from the fire within and speeds up the fire process. This could influence evacuation negatively, with both higher temperatures and more smoke than an equal fire in a less insulated building. The insulation capacity of textile membranes is less than any conventional building material element, except uninsulated steel (20). For evacuation safety in a fire scenario this is mostly a bad quality. However, for the types of buildings for which textile membranes are used low insulation capacity might improve the evacuation situation. The heat and smoke build up will be slower, the radiation less and thus, there will be more time to evacuate.

Insulation is very important to limit the spread of smoke and fire from one part of a building to another or between buildings. Textile membranes does probably not make good fire compartments. This might complicate the fire services job to confine and limit the damage to parts of a fire ravaged building. Textile membranes would not work as the dominant building material for buildings in more than one floor with complex emergency routs, such as offices, hospitals or housing estates.

3.2.7 Combustion products, toxic gases and smoke production

A great part of the people killed in building fires die from the smoke and not from the heat. This means that the combustion products the building material will give away when heated or burned must be taken into consideration when designing a buildings fire prevention. As described in 3.1 above many polymers give away toxic gases when burned.

The amount of combustion products is limited by the amount of building material available for combustion. In buildings of textile membranes this supply of combustible material is very limited. For example, the test building in Chapter 1 would contain about four times as much combustible material if it was built up of thin fibreboard (3,2 mm (20)) instead of textile membrane (0,5 mm). And if it was build up as a conventional house the difference would be even greater. The toxic gases need to be confined in a limited space to have effect on people. I.e. to quantify the dangers with combustion products in a building fire, not only the toxicity of the combustion products has to be taken into consideration but also the amount of combustible material available and the volume of air in the building that the toxic gases can mix with. Textile membranes probably produce gases with a higher toxic effect than conventional building materials such as concrete, wood, brick, plaster (board) and steel. However, the amount of material is substantially less and when the gases are produced the material will burn away and create ventilation which will somewhat lower the rate of toxicity, depending on the geometry.

3.2.8 Summation

To conclude, there are a lot of risks that need to be addressed when working with buildings of textile membranes. Some of these differ considerably from the corresponding risks that would occur in a building of conventional materials. Some of the risks discussed above are: burning droplets, fallings parts, collapse of the building, rapid flame spread, no confinement of the fire to limited parts of the building.

This risk identification illuminates a lot of different risks and opens up a lot of interesting areas of research. This thesis will however only focus on the burning away and hole opening of the textile membrane and these phenomenon's impact on the evacuation of the building.

4 Validation experiments

The validation experiments were conducted at the Swedish Technical Research Institute (SP) in Borås.

4.1 Test set-up

For validation a total of four full scale tests, two with each of the two membranes, were conducted by SP in Borås. The tests were conducted in rooms of standardized ISO 9705 room size (Figure 5), 2.4 m in height, 2.4 m in width and 3.6 m in length. Three of the walls and the roof were made of the tested membrane and the wall with the door opening of a unburnable board, Promatect. The membrane was mounted on a steel frame. (1)

The whole room was placed under a calorimetric hood (Figure 5), smoke production and heat release rate (HRR) could thus be measured. The experiments were photographed every ten seconds. Time to hole were noted. After each experiment the size of the hole was measured. (21)

Figure 5. The test set-up for the large-scale tests with textile membranes conforming to the size of the ISO 9705 room, 2.4 m × 2.4 m × 3.6 m (left), and the position of the burner in the centre of the room in one of the validation experiments (right). (1)

The burner was a sand burner with the dimensions 0.3 m x 0.3 m placed in the middle of the room at two different heights, 0.45 m and 1 m above the floor, see Figure 5 and table 1.

Table 1. Test description. (21)

Test	Textile membrane	Burner location	Burner stages	Notes on burn-through
7	B8103/ PVC-PES	1.0 m above floor	95 kW – 5 min 140 kW – 5 min	Burn-trough during 95 kW exposure
8	B8103/ PVC-PES	0.45 m above floor	95 kW – 10 min 140 kW – 10 min 300 kW – 5 min	Burn-trough during 300 kW exposure
9	T3107 / PVC-PES	1.0 m above floor	95 kW – 5 min 140 kW – 5 min	Burn-trough during 95 kW exposure
10	T3107/ PVC-PES	0.45 m above floor	95 kW – 10 min 140 kW – 10 min 300 kW – 5 min	Burn-trough during 300 kW exposure

Temperature and velocities were measured in the door frame every ten cm from zero to one m below the soffit. The temperature in the room was measured by a thermocouple tree placed 0.8 m from the rear wall and 1.2 m from each side wall. It measured the temperature every ten cm from 0.1 – 2.3 m above the floor. The temperatures obtained in the door and room has been important in estimating the thickness of the smoke layer.

Two thermocouples were mounted directly on the roof membrane in the centre of the room, one on the inside and one on the outside. These two thermocouples tend to give strange values because they are placed directly in the flame and they fall down from the roof as soon as a hole opens up. A plate thermocouple was placed on the floor in close proximity to the thermocouple tree. A simple optical smoke measurement device was positioned between the thermocouple tree and the burner 1.6 m above ground.

5 Fire Dynamics Simulator (FDS)

Fire Dynamics Simulator (FDS) is a computational fluid dynamics model. The software solves Navier-Stokes equations and is well suited for simulating low speed thermally-driven flows such as those produced by fire and smoke. The turbulence is calculated with the Smagorinsky form of Large Eddy Simulation (LES). FDS is widely used for performance based fire safety design. It reads input parameters from a text file, computes according to the governing equations and writes the sought data to files. The program includes several sub-models for modelling combustion, radiation, water droplet trajectories, heat transfer, pyrolysis and so on. (7) FDS is under constant development and the latest version, version 5.5.0 was released in April 2010.

Version 5.4.3 of FDS has been used to simulate the experiments. The serial (single processing) version has been used without exceptions, due to the size of the room and positioning of the burner. The risk concerning loss of data between meshes is too high for parallel processing. Simulations has been performed on different computers for practical reasons and to secure the validity of the program. Both Linux (CentOS 5.3 x86_64) and Windows Vista (Home & Ultimate versions) gave the same results, as did the different setups in CPU architecture (32-bit & 64-bit) and CPU/Memory capacity between computers. See Appendix A – System specifications for information on the different systems used.

The model for radiative heat transfer has been used consistently in the simulations. Wide band model has not been used, why the default radiation transport equation for a gray gas was calculated. The equation is solved using a technique similar to finite volume methods for convective transport, thus the name given to it is the Finite Volume Method (FVM). The solver requires about 20 % of the total CPU time if 100 discrete angles is used. The number of angles used in all simulations is 104, which is the default value. RADCAL narrow-band model is used to calculate the absorption coefficients of the gas-soot mixtures.

To visualize the results the software Smokeview is used to read the data and produce pictures from it. While Smokeview has a user interface FDS does not, the code is written directly into a text document. There are however some programs, like the commercial Pyrosim, which helps the user create the FDS input via an interface. Some of the features of Pyrosim is a number of drawing tools, the constant view of the geometry and the possibility to import 2D and 3D AutoCAD DXF files or existing FDS files (22). The importing feature is especially usable when dealing with complex geometries which would be both time consuming and difficult to write manually in a text file. However, Pyrosim does not have all the advanced settings, like bulk density, which are required for the project. Therefore Pyrosim was only used to import the complex geometries.

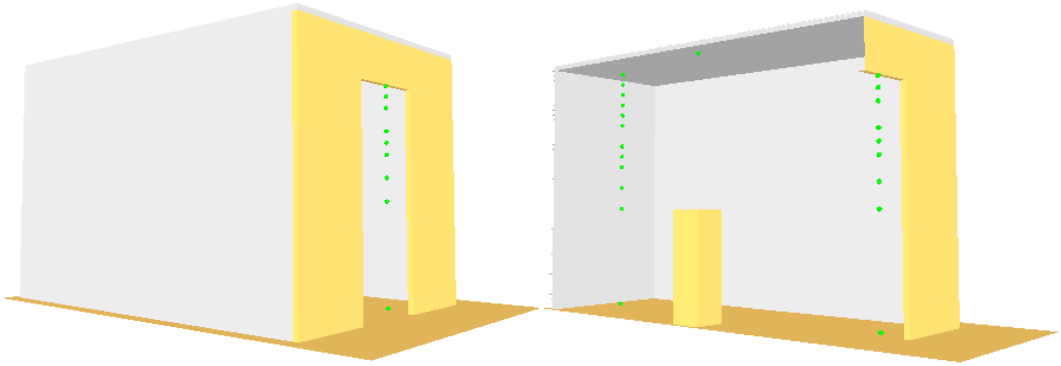

Figure 6. Smokeview picture of the geometry in FDS.

The green dots in Figure 6 above are devices measuring temperature. These are placed in the same places as the devices in the validation experiments. A thermocouple tree in the rear, a tree in the door, one thermocouple in the ceiling and one on the roof directly opposite. The burner, measuring 0,30 by 0,30 m, is placed on the column in the middle of the room.

5.1 The burn away option

The burn away option was used to mimic the opening of a hole in the roof of a building made of textile membrane. When using the burn away option in FDS a cell is removed from the calculation as soon as it is exhausted of fuel by the pyrolysis reactions or by the prescribed HRR. The material will burn away one cell at a time until the simulation stops, all of the material is burned away or the temperature is too low for further burning away (depending on the input configuration).

Burn away is a coarse simplification of a very complicated process. In a real fire, a hole can arise from a number of reasons or a combination of some, such as pyrolysation or burning off, but also melting of the material or because of local weaknesses in the material. The burn away option does not account for the latter two.

5.2 Pyrolysis models

The choice of pyrolysis model depends largely on what properties one can find to describe the material in question. During the course of the work two different pyrolysis models has been used: Solid Fuels that burn at a specified rate (called model I)and Solid Fuels that do NOT Burn at a Specified Rate (called model II). (7)

5.2.1 Model I: Solid Fuels that Burn at a Specified Rate

This pyrolysis model uses a prescribed burn rate, where the material disappears with heat release per unit area (HRRPUA) when the ignition temperature is reached at the surface. When using this pyrolysis model the parameters ignition temperature (IGNITION_TEMPERATURE) and heat release rate per unit area needs to be prescribed. The membrane will neither burn nor pyrolyse before it reaches the ignition temperature. When this temperature is reached it will immediately burn of at the rate prescribed by HRRPUA. If ignition temperature is not prescribed the burn rate will immediately go to HRRPUA when the simulation starts. When specifying the HRRPUA parameter the burning rate is controlled instead of letting it depend on the surroundings. There is a possibility to “ramp” the burning linearly if prescribing command lines similar to:

```
&RAMP ID    = 'fire_ramp',    T    = 0.0,       F    =0.0 /
&RAMP ID    = 'fire_ramp',    T    = 20.0,      F    =1.0 /
&RAMP ID    = 'fire_ramp',    T    = 620.0,     F    =1.0 /
&RAMP ID    = 'fire_ramp',    T    = 640.0,     F    =0.0 /
```

If this command is given and connected to the function which controls surface properties (surf) the burning will ramp linearly from the point where the temperature of ignition is reached up to full effect (HRRPUA) in 20 seconds. It will then burn for ten minutes and ramp down for another 20 seconds. Note that T is time from ignition. (7) This feature has not been used because it is hard to guess what times are appropriate for the ramping.

The parameter HEAT_OF_VAPORIZATION can also be added to the surf line. This tells FDS to account for the energy loss in the surrounding material due to the vaporization of the fuel. If it is not given there will be no link between burning rate and surface temperature and the material may heat up too much. This parameters influence on the results was judged to be marginal, since the small mass gives a very limited energy content of the membrane in relation to the burner output. The parameter was not included. Also there are no experimental values for heat of vaporization for plastics due to the complexity of their vaporization. The term used for plastics is decomposition. More on this in chapter 3.1 and under heat of reaction in 5.3.

An example from our input files follows:

```
&MATL ID                    = 'PVC',
SPECIFIC_HEAT               = 0.97,
CONDUCTIVITY                = 0.23,
DENSITY                     = 1045/

&SURF ID                    = 'PVC-SHEET-A',
MATL_ID                     = 'PVC',
COLOR                       = 'GRAY 80',
HRRPUA                      = 4.,
BURN_AWAY                   = .TRUE.,
IGNITION_TEMPERATURE        = 200.,
BACKING                     = 'EXPOSED',
THICKNESS                   = 1.1e-003/
```

5.2.2 Model II: Solid Fuels that do NOT Burn at a Specified Rate

This pyrolysis model does not use a prescribed rate but instead an Arrhenius like reaction rate. This model lets you specify a number of different reactions for the material, such as vaporization, gasification of different species in the material and so on. However, only one reaction (the pyrolysation) has been simulated. If results from a thermo gravimetric analysis (TGA) exists, one can use the parameters REFERENCE_TEMPERATURE and PYROLYSIS_RANGE to calculate A and E for the Arrhenius reaction. If these are given the pyrolysation process will accelerate from the reference temperature minus half of the pyrolysis range according to the Arrhenius function.

Used reference temperature and pyrolysis ranges in the simulations are derived from a thermo gravimetric analysis, see explanation under 5.3 and in Appendix B – TGA results. Reference temperature is the temperature where the burn rate peaks and pyrolysis range is the width in degrees Celsius under which the pyrolysation takes place in a standardized TGA test.

If specified in this model the reaction can produce solid residue, water vapour and/or fuel gas. To use this, one must specify some parameters for the residue. The function has been tried with the following lines, where residue is called ash:

```
&MATL ID                = 'PVC',
SPECIFIC_HEAT           = 0.97,
CONDUCTIVITY            = 0.23,
DENSITY                 = 1300,
REFERENCE_TEMPERATURE   = 280.,
PYROLYSIS_RANGE         =160.,
N_REACTIONS             =1,
NU_FUEL                 = 0.85,
NU_RESIDUE              = 0.15,
RESIDUE                 = 'ASH'/

&MATL ID                = 'ASH'
DENSITY                 = 1300,
SPECIFIC_HEAT           = 1,
CONDUCTIVITY            = 0.2/
```

If the properties of the residue is unknown one can use only the NU_FUEL line. As this is the case the final method to emulate residue is to set NU_FUEL to 0,85 without creating a new residue material. In the following case 85% of the solid will become fuel gas.

```
&MATL ID                = 'PVC',
SPECIFIC_HEAT           = 0.97,
CONDUCTIVITY            = 0.23,
DENSITY                 = 1300,
REFERENCE_TEMPERATURE   = 280.,
PYROLYSIS_RANGE         = 160.,
N_REACTIONS             = 1,
NU_FUEL                 = 0.85/
```

See Appendix E – Variation of parameters for different test with residue. In most of the simulations no residue was used. An example from our input files follows:

```
&MATL ID                 = 'PVC',
SPECIFIC_HEAT            = 0.97,
CONDUCTIVITY             = 0.23,
DENSITY                  = 1300,
REFERENCE_TEMPERATURE    = 280.,
PYROLYSIS_RANGE          = 160.,
N_REACTIONS              = 1,
NU_FUEL                  = 1/
&SURF ID                 = 'PVC-SHEET-A',
MATL_ID                  = 'PVC',
COLOR                    = 'GRAY 80',
BURN_AWAY                = .TRUE.,
BACKING                  = 'EXPOSED',
THICKNESS                = 5.0e-004/
```

5.3 Input in FDS – Material parameters

The parameters used are described from the method used to quantify them. Two membranes were tested, see table 2. Some of the material parameters used were given by the manufacturer of the membranes while some had to be determined with tests in the cone calorimeter, TGA or TPS.

Table 2. Materials and values given by the manufacturer.

Material	Density [kg/m^3]	Thickness [mm]
Sioen B8103/ PVCPES	1300	0,5
Sioen T3107 / PVCPES	1045	1,1

Cone calorimeter

Tests in the cone calorimeter (23) were conducted by SP Technical Research Institute of Sweden to provide some of the input parameters needed for the FDS simulations.

Ignition temperature
The temperature at which the membrane is set to ignite was set after cone calorimetric tests with a thermocouple attached to the membrane.

Heat of combustion
The energy released per unit mass of fuel gas combusted. A mean value from two separate tests with 0,5 mm membranes was calculated to 1434 kJ/kg. In the final simulations 1400kJ/kg was used in conjunction with this membrane .

The test value for the 1,1 mm membrane was 2054 kJ/kg. In the final simulations with the this membrane 2100 kJ/kg was used.

HRRPUA - Heat Release Rate Per Unit Area
Specifies the heat released from the membrane per unit area when the temperature of ignition is reached. At temperatures under ignition temperature, HRRPUA equals zero. This parameter is only used in pyrolysis model I.

TGA

Tests in the Thermo Gravimetric Analyser were conducted by SP Technical Research Institute of Sweden to provide some of the input parameters needed for the FDS simulations. The TGA results is presented in Appendix B – TGA results.

Reference Temperature
The reference temperature is defined as the peak of the mass fraction curve in an TGA, see Appendix B – TGA results. This means the temperature at which the mass fraction decreases at its maximum, i.e. the burn rate peaks. This temperature is not the same as the ignition temperature or the surface temperature of the burning material. (7)

Pyrolysis range
The pyrolysis range is the approximate width (ΔT) of the temperature range during which the major part of the mass burns off in an Thermogravimetric Analysis. The pyrolysis range is centered around the reference temperature. (7) The range is derived from results presented in Appendix B – TGA results.

Residue
Simply the solid residue from the burning of a solid material, represented as a mass fraction of the starting mass. The values for the membranes are derived from results presented in Appendix B – TGA results.

TPS

Tests in the Transient Plane Source (24) was conducted by SP Technical Research Institute of Sweden to provide some of the input parameters needed for the FDS simulations.

Conductivity
The property that indicates a materials ability to conduct heat. Thermal conductivity is measured in watts per K per meter (W/Km).

Specific heat
The amount of energy needed to raise the temperature of the membrane. Specific heat is measured in kJ/kgK.

External references

Radiative fraction
The fraction of energy released from the fire as thermal radiation. The fuel used in the simulations is propane, which also is the default fuel in FDS (7). The default radiative fraction 0,35 is therefore chosen. This value also coincides with the one given in SFPE (25).

Bulk density
The input parameter bulk density is needed to solve two problems. FDS can only handle combustion of one gaseous fuel hence the problem since the combustion of propane is not identical with the combustion of the textile membranes. There is also the problem with the thickness of the membrane (0,5 and 1,1 mm) that does not agree with the grid size of 5, 10 or 20 cm, since burn away does not account for the thickness parameter. It can only burn away whole cells of material. Bulk density calculates the density that should be prescribed to the membrane on the &OBST line to take care of these problems. In the formulae below the density is the density of the membrane and HC is the heat of combustion.

$$\text{Bulk density} = \text{density} / \left(\frac{\text{HC}_{\text{propane}}}{\text{HC}_{\text{membrane}}} * \frac{\text{gridsize}}{\text{membrane thickness}} \right)$$

Incombustible board
The board that makes up for the front wall in the experiments and simulations is defined with parameters that makes it incombustible. It is named unburnable in the input file.

Heat of reaction
A parameter associated to pyrolysis model II. No extensive testing has been performed on this parameter because of shortage of time and due to the uncertainties concerning the definition of the parameter. The user guide (7)defines the heat of reaction as the amount of energy consumed per unit mass of reactant that is converted into something else i.e. the enthalpy difference between the products and the reactant. See discussion in chapter 8.2 and Appendix E – Variation of parameters for used values and results.

5.4 Input parameters used

In table 3 and table 4 below the most reasonable parameter values from reliable sources are accounted for. Generally they give the best results, although not always. For more input parameters used see Appendix E – Variation of parameters.

Table 3. Input parameters for model I, 5 cm grid size.

Test	7	8	9	10
Parameter				
Density [kg/ m^3]	1300	1300	1045	1045
Thickness [mm]	0,5	0,5	1,1	1,1
Conductivity [W/m·K]	0,23	0,23	0,23	0,23
Specific Heat , Cp[kJ/kg.K]	0,97	0,97	0,97	0,97
HRRPUA [kW/m^2]	10	10	10	10
Heat of Combustion, ΔH_c [kJ/kg]	1400	1400	2100	2100
Radiative fraction	0,35	0,35	0,35	0,35
Ignition Temperature [°C]	200	200	200	200
Bulk density [kg/m^3]	0,385	0,385	1,02	1,02

Table 4. Input parameters for model II, 5 cm grid size.

Test	7	8	9	10
Parameter				
Density [kg/ m^3]	1300	1300	1045	1045
Thickness [mm]	0,5	0,5	1.1	1,1
Conductivity [W/m·K]	0,23	0,23	0,23	0,23
Specific Heat , Cp[kJ/kg.K]	0,97	0,97	0,97	0,97
Heat of Combustion [kJ/kg]	1400	1400	2100	2100
Radiative fraction	0,35	0,35	0,35	0,35
Reference Temperature [°C]	280	280	280	280
Pyrolysis range [°C]	80	80	80	80
Fuel [fraction]*	0,85	0,85	0,85	0,85
Bulk density [kg/m^3]	0,385	0,385	1,02	1,02

*85% of the fuel is combusted, the rest is residue.

6 Results

In this chapter a selection of simulation results are accounted for and compared with other simulations and with the validation experiments. See Appendix E – Variation of parameters for a list over some of the simulations done. All figures show simulations for the finer grid size, 5 cm, if nothing else is mentioned.

6.1 Pyrolysis Model I

Figure 7 through Figure 9 below show the temperatures from the rear thermocouple tree at 2,3 m above the floor compared to temperature devices at the same location in a number of simulations. In Figure 7 the green curve shows the best agreement with the experimental temperatures.

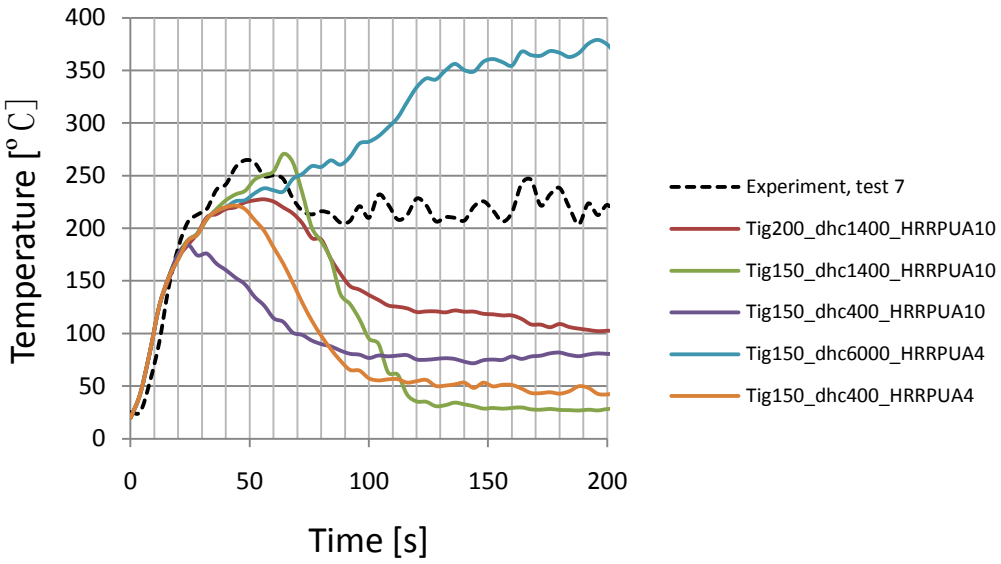

Figure 7. Test 7. Experiment compared to simulations with variations in ΔHc and HRRPUA. See Table 8 in Appendix E – Variation of parameters.

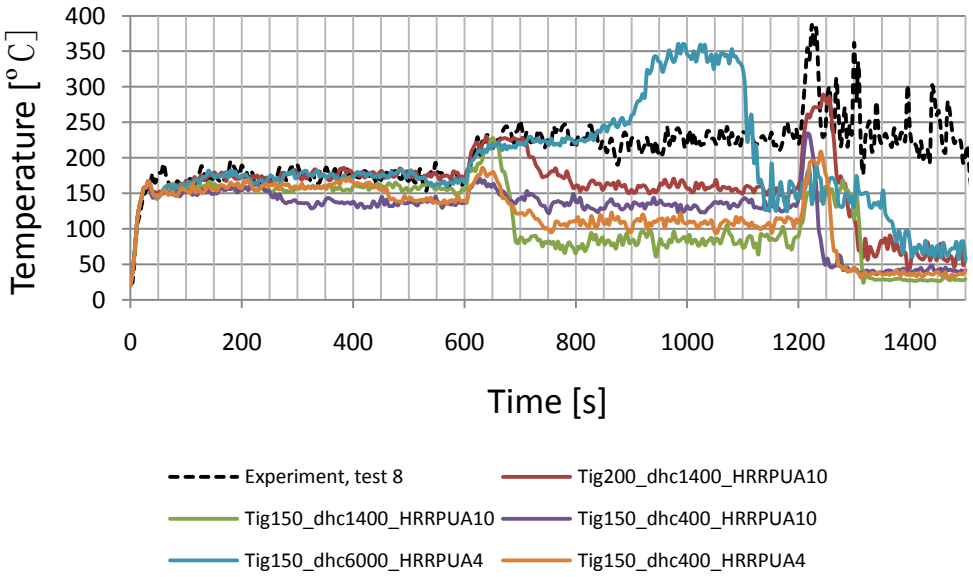

Figure 8. Test 8. Experiment compared to simulations with variations in ΔHc and HRRPUA. See Table 9 in Appendix E – Variation of parameters.

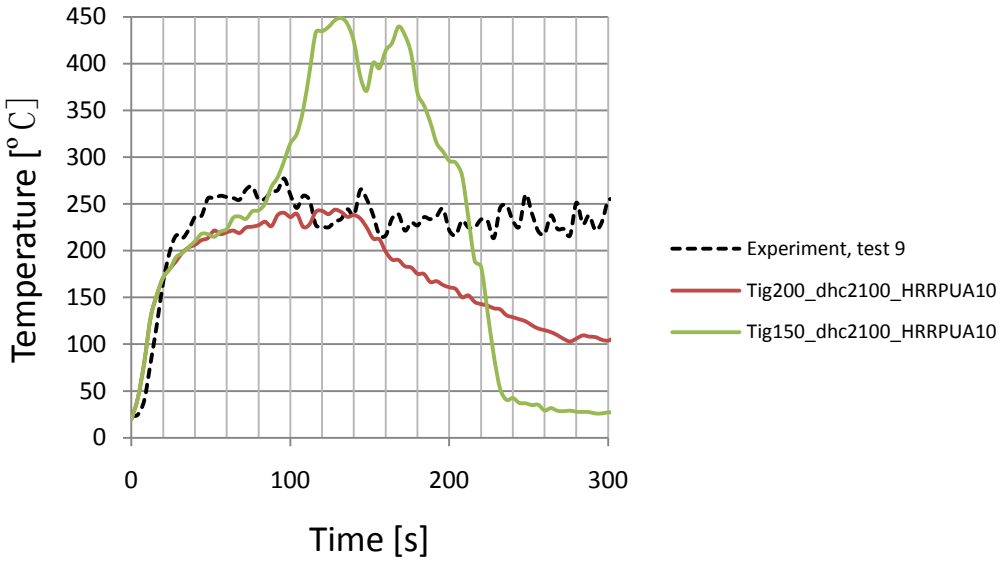

Figure 9. Test 9. Experiment compared to simulations with variations in ΔHc and HRRPUA. See Table 10 in Appendix E – Variation of parameters.

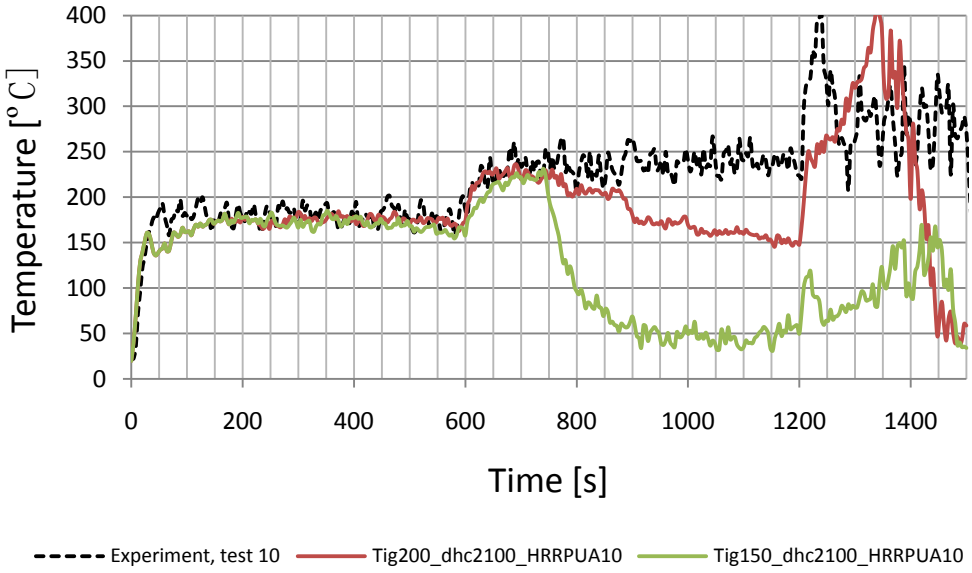

Figure 10. Test 10. Experiment compared to simulations with variations in ΔHc and temperature of ignition. See Table 11 in Appendix E – Variation of parameters.

Figure 11 below is made up of two captions (snapshots) from Smokeview. The left picture represents the moment where the ceiling is at its highest temperature. After this some of the cells will cool down to a temperature under 150°C. The right picture shows the end of the simulation and indicates that all cells which has at some point reached 150°C will eventually burn away. This shows that the HRRPUA works as a ON button when the cells temperature reaches the set ignition temperature.

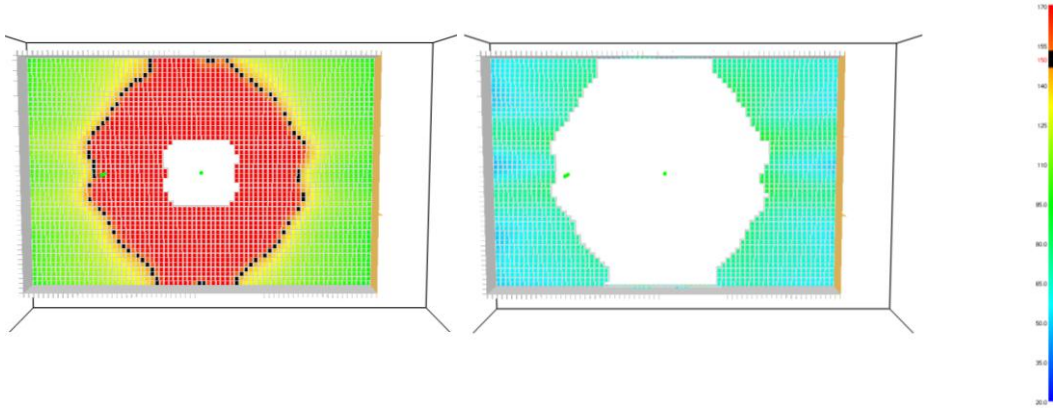

Figure 11. Test 7, model I, ignition temperature 150°C, after 62 and 600 seconds. Black indicates 150°C and every cell within is hotter.

Figure 12 below shows the same results as above but for temperature of ignition 200°C. Apart from this difference the two input files are identical. The caption to the upper left in Figure 12 shows the largest area of the roof that reaches the ignition temperature with the initial burner effect. The right caption shows the largest area that reaches the ignition temperature with the increased burner effect. The lower left caption shows the final hole. The hole is clearly influenced by the ON function.

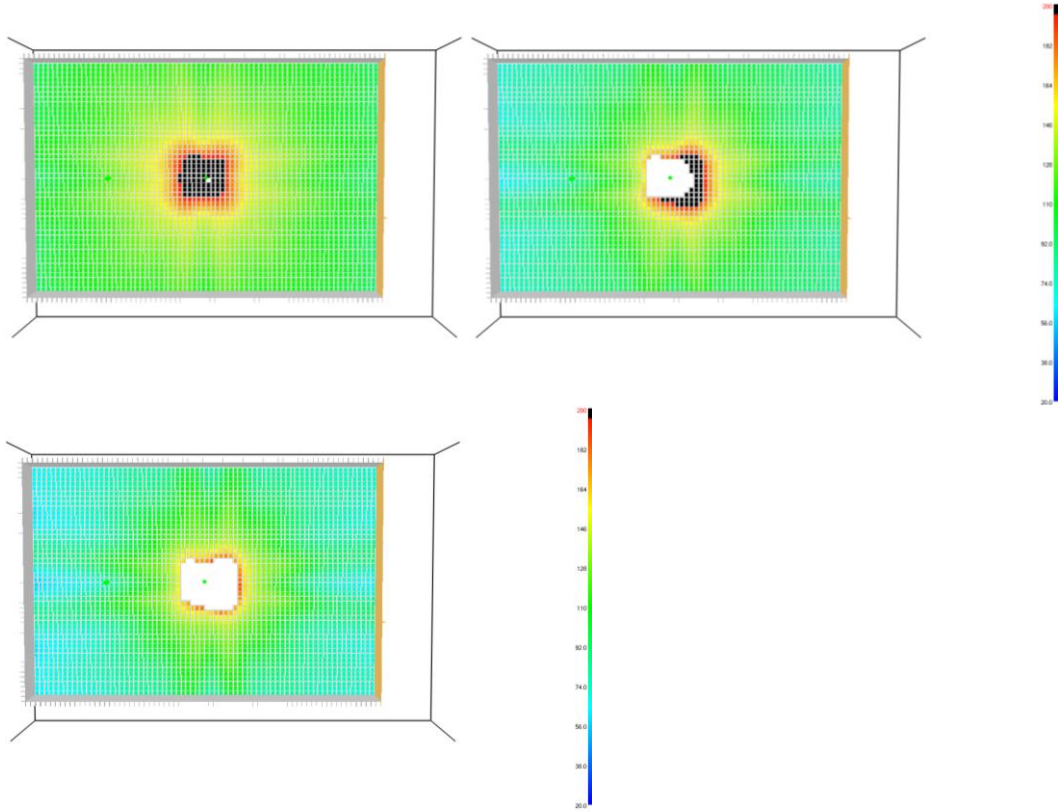

Figure 12. Test 7, model I, ignition temperature 200°C, after 54,6; 341,4 and 447 seconds. Black indicates 200°C and every cell within is hotter.

6.1.1 Grid independency for Pyrolysis Model I

Because of the computer capacity and calculation time needed to run FDS simulations it is of high importance to find the line between result quality and time saving. For example, reducing the cell size in half for test seven increased the simulation time by a factor of 17. The term grid independence means that one refines the grid until no appreciable differences in the simulation results can be

detected, i.e. the results are independent of the grid size. It is not clear if grid independence has been reached because only two grid sizes has been used and they showed differences. See Appendix E – Variation of parameters for a list over some of the simulations done.

For simulations involving buoyant plumes one can estimate how well the plume is resolved with the relationship between the so called characteristic fire diameter and the grid size, see Appendix C – Characteristic diameter of the fire. The smaller the fire diameter and the greater the heat release rate, the more cells spanning the fire is needed. (7)

Figure 13 through Figure 16 below shows the differences in flame height and resolution of the flame between the grid sizes at different times during the simulation. Figure17 and Figure 18 shows the flame temperature difference between the grid sizes twelve seconds after simulation start. All figures shows a cross section approximately through the middle of the simulated ISO-room.

For the simulations showed in Figure 13 and Figure 14 below the first cells in the ceiling reaches temperature of ignition after 16,5 s (5 cm grid) and 166,5 s (10 cm grid). This is a very good example of how better solution leads to higher temperatures. See also Figure 13 through Figure 18 and Figure 23 and Figure 24 for additional pictures and further discussion under chapter 8.

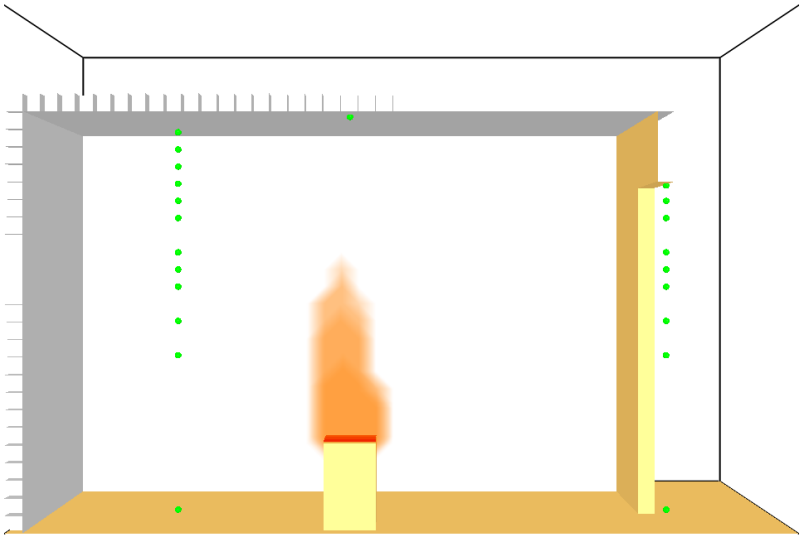

Figure 13. Test 8, ignition temperature 150° C, 10cm grid size, after 12 seconds, flame > 200kW/m³.

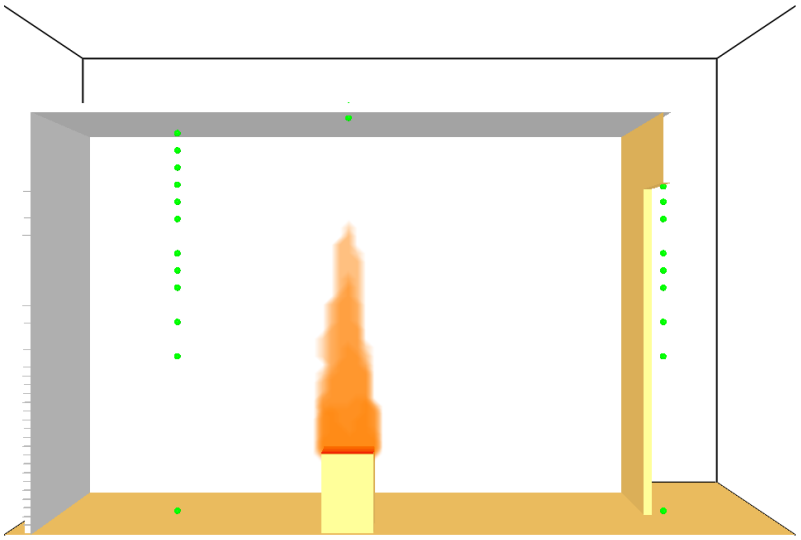

Figure 14. Test 8, ignition temperature 150° C, 5 cm grid size, after 12 seconds, flame > 200kW/m³.

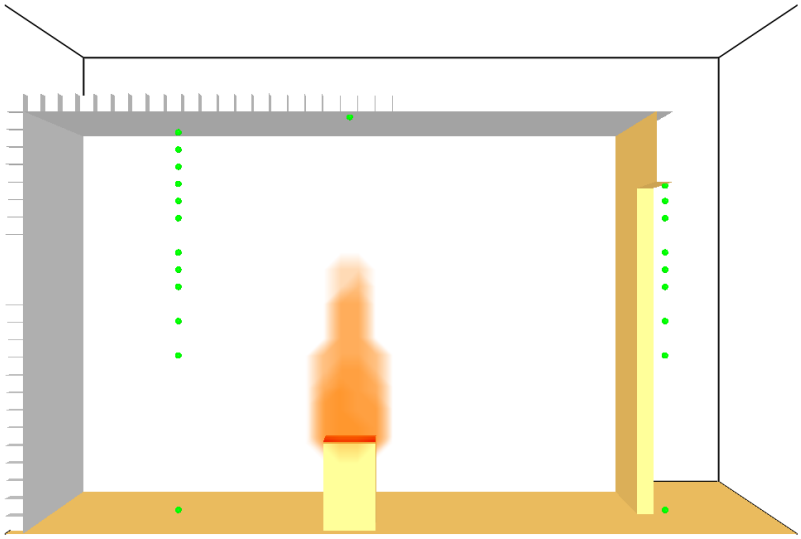

Figure 15. Test 8, ignition temperature 150° C, 10 cm grid size, after 100,5 seconds, flame > 200kW/m³.

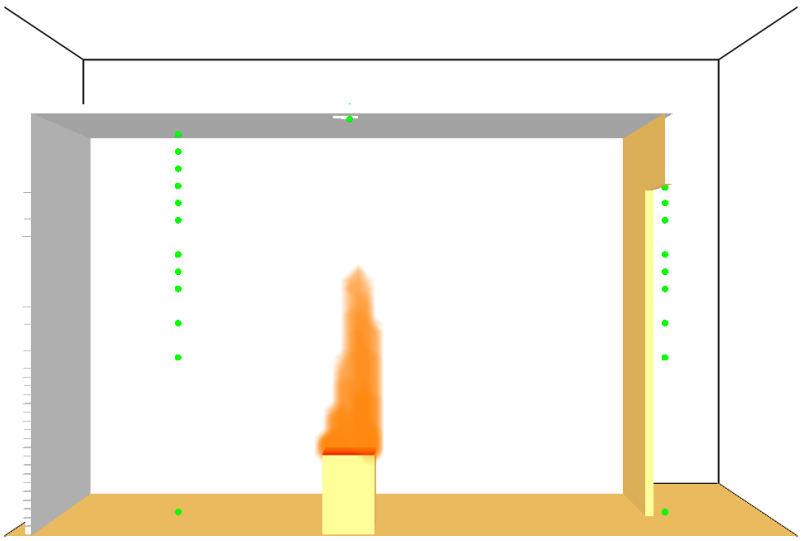

Figure 16. Test 8, ignition temperature 150° C, 5 cm grid size, after 100,5 seconds, flame > 200kW/m³.

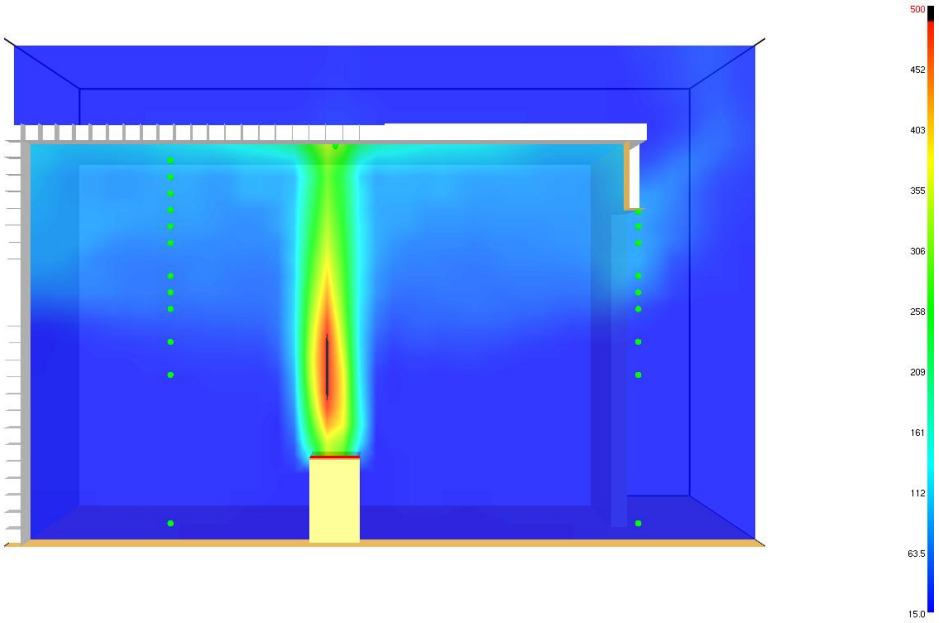

Figure17. Test 8, ignition temperature 150, 10cm grid size, after 12 seconds. Slice file temperature, 500° C marked black.

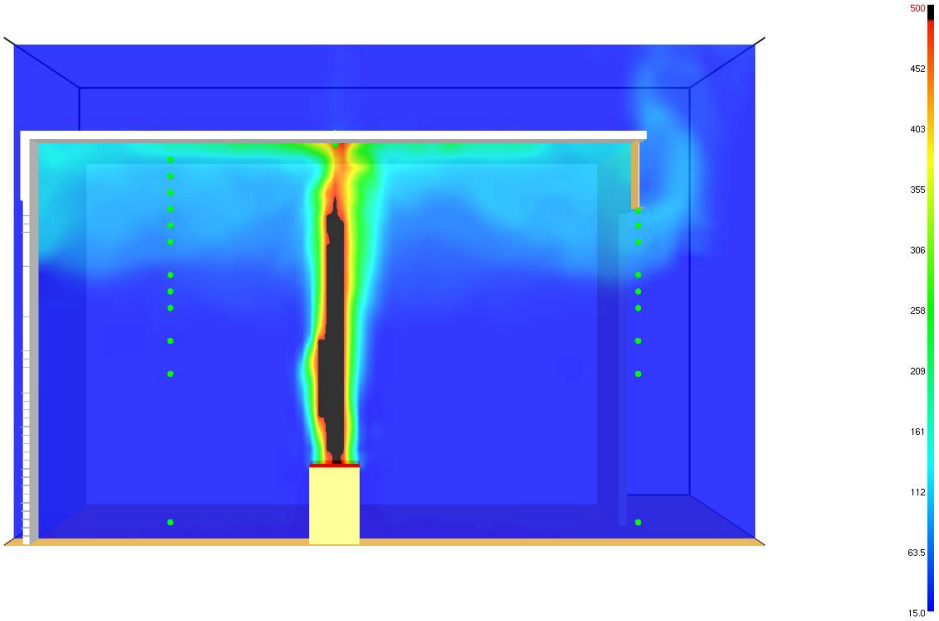

Figure 18. Test 8, ignition temperature 150, 5 cm grid size, after 12 seconds. Slice file temperature, 500° C marked black.

6.2 Pyrolysis Model II

As the results, for tests eight and ten, with pyrolysis model I did not coincide with the validation experiments it was decided to make some attempts using a different pyrolysis model, see pyrolysis model II, 5.2.2. See Appendix E – Variation of parameters for a list over some of the simulations done.

Figure 19 - Figure 22 below shows the temperatures in the rear thermocouple tree at 2,3 m above the floor compared to temperature devices at the same location in a number of simulations.

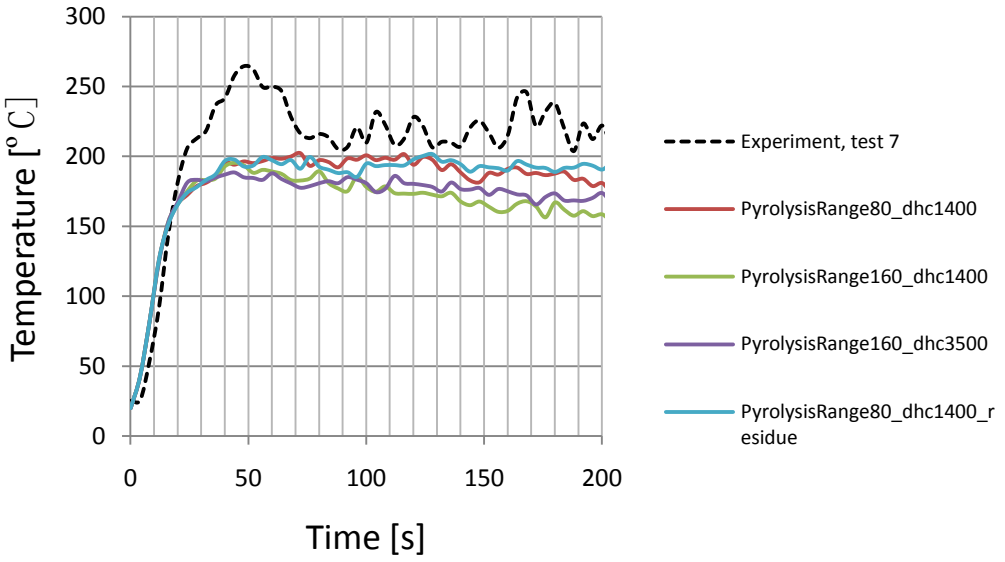

Figure 19. Test 7. Experiment compared to simulations with variations in residue, ΔHc and pyrolysis range. See Table 12 in Appendix E – Variation of parameters.

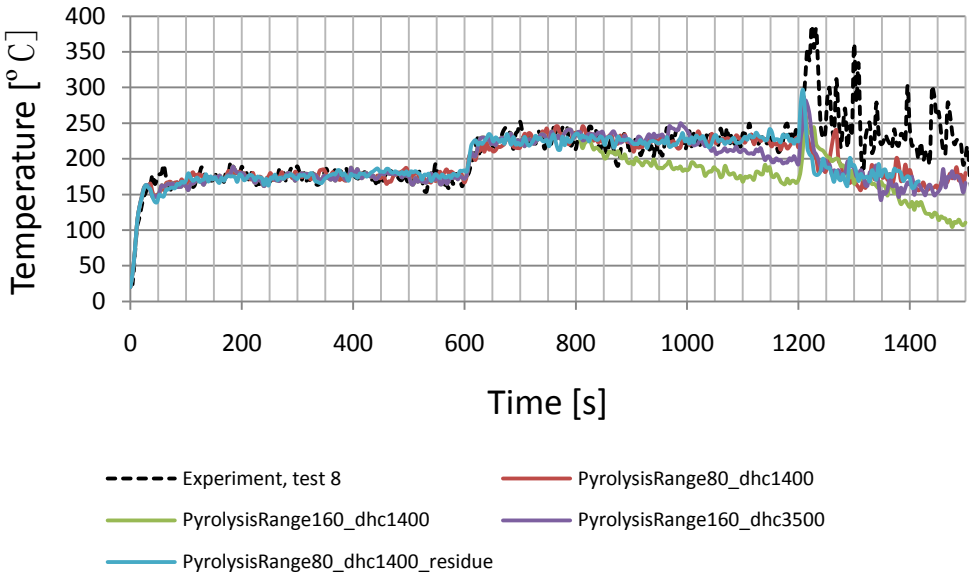

Figure 20. Test 8. Experiment compared to simulations with variations in residue, ΔHc and pyrolysis range. See Table 13 in Appendix E – Variation of parameters.

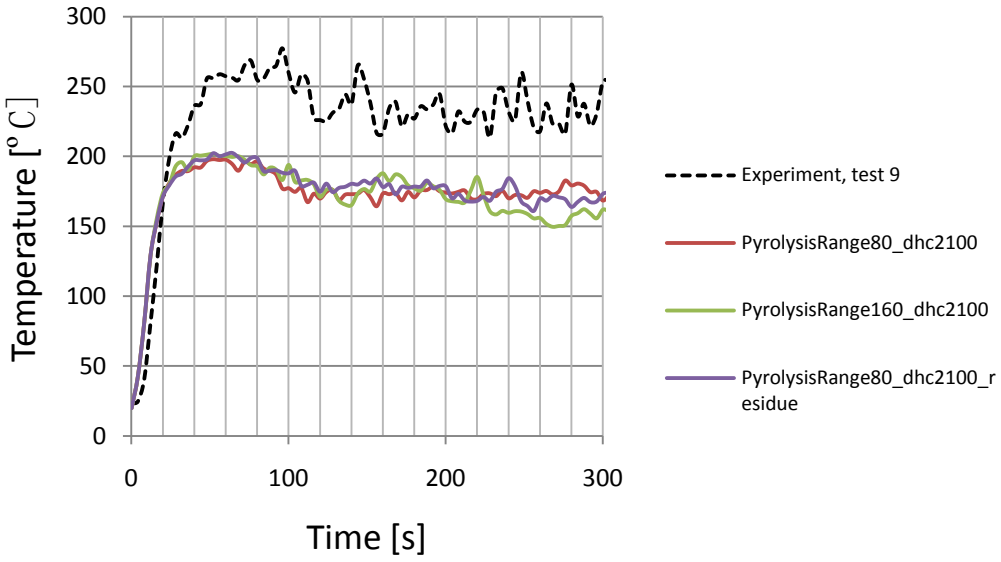

Figure 21. Test 9. Experiment compared to simulations with variations in residue and pyrolysis range. See table 14 in Appendix E – Variation of parameters.

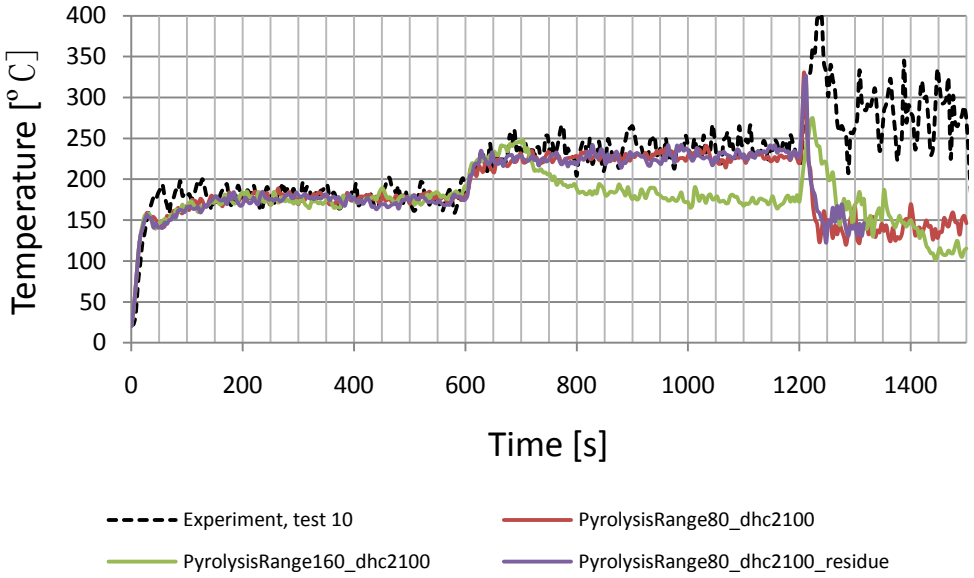

Figure 22. Test 10. Experiment compared to simulations with variations in residue and pyrolysis range. See

Table 15 in Appendix E – Variation of parameters.

6.2.1 Grid independency for Pyrolysis Model II

As with model I, it is not clear if grid independence has been reached because only two grid sizes has been used and they showed differences, see Table 12 - Table 15 in Appendix E. Figure 23 below shows the difference in flame height and resolution of the flame between the grid sizes for test seven 15 seconds after simulation start. Figure 24 shows the flame temperature difference between the grid sizes for test seven 15 seconds after simulation start. Figure 25 shows the air flows and turbulence in test seven at a time when steady state has been reached. Figure 26 and Figure 27 shows the air flows and turbulence in test eight before and after hole has been opened. All figures shows a cross section approximately through the middle of the simulated ISO-room.

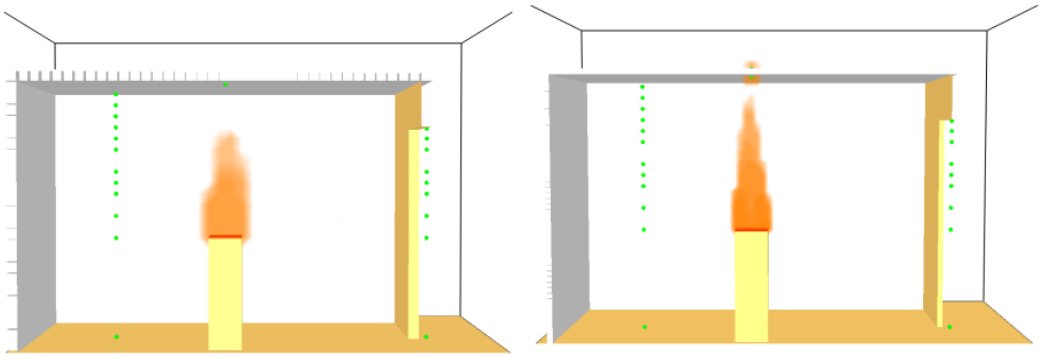

Figure 23. Test 7. The difference in flame height between 10 cm grid size (left) and 5 cm grid size (right). , flame > 200kW/m3

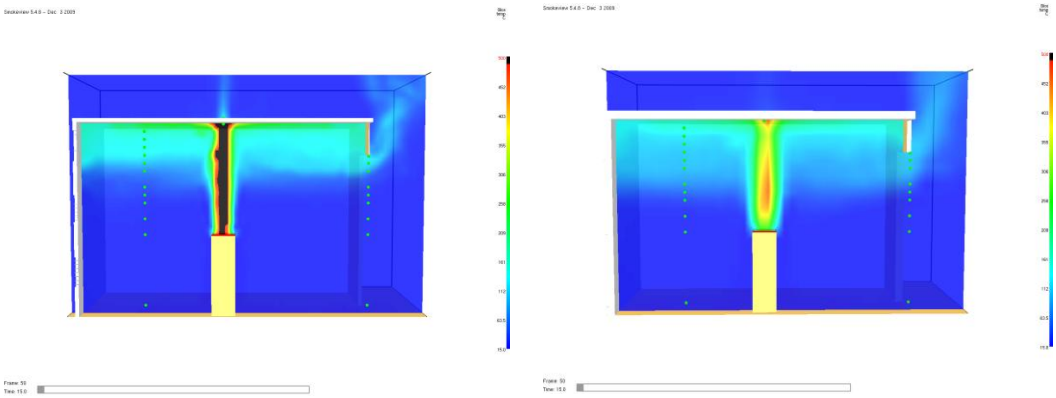

Figure 24. Test 7, after 15 seconds. The difference in plume temperature in test 7 between 10 cm grid size (right) and 5 cm grid size. In both figures 500ºC marked black. In the right one the plume does not reach this temperature but in the left a solid plume from burner to ceiling is at least this temperature.

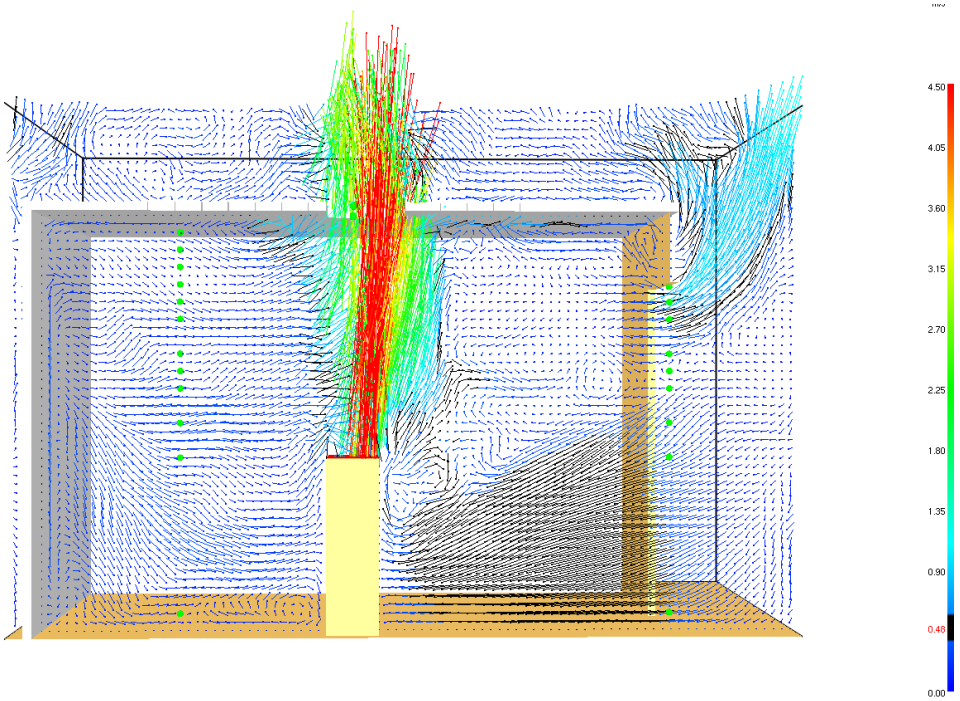

Figure 25. Test 7, after 600 seconds, hole, 5 cm grid size. The effect of air entrainment on the plume. Red indicates a air velocity of 4,5 m/s.

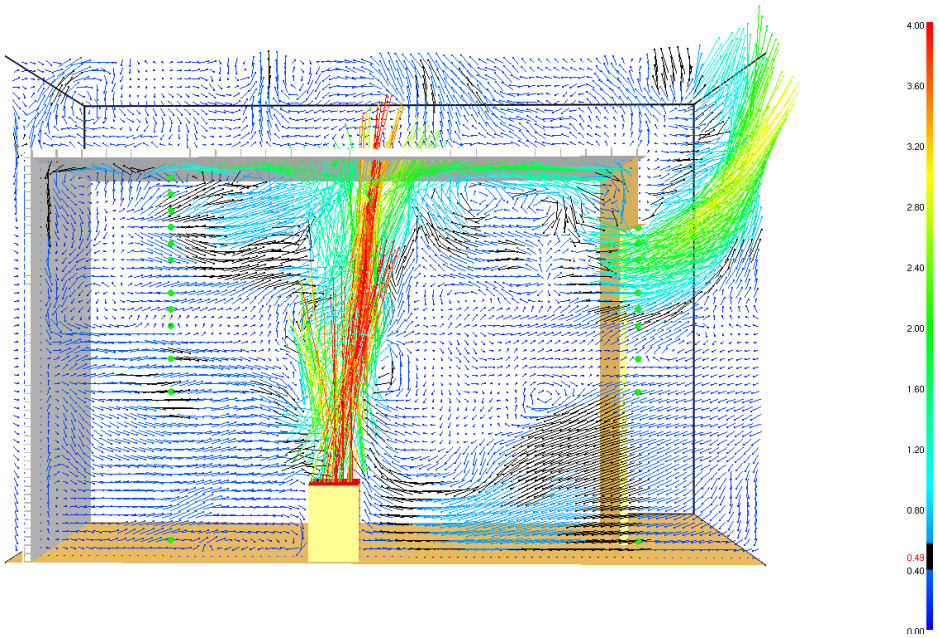

Figure 26. Test 8, after 600 seconds, no hole, 5 cm grid size. The effect of air entrainment on the plume. Red indicates a air velocity of 4 m/s.

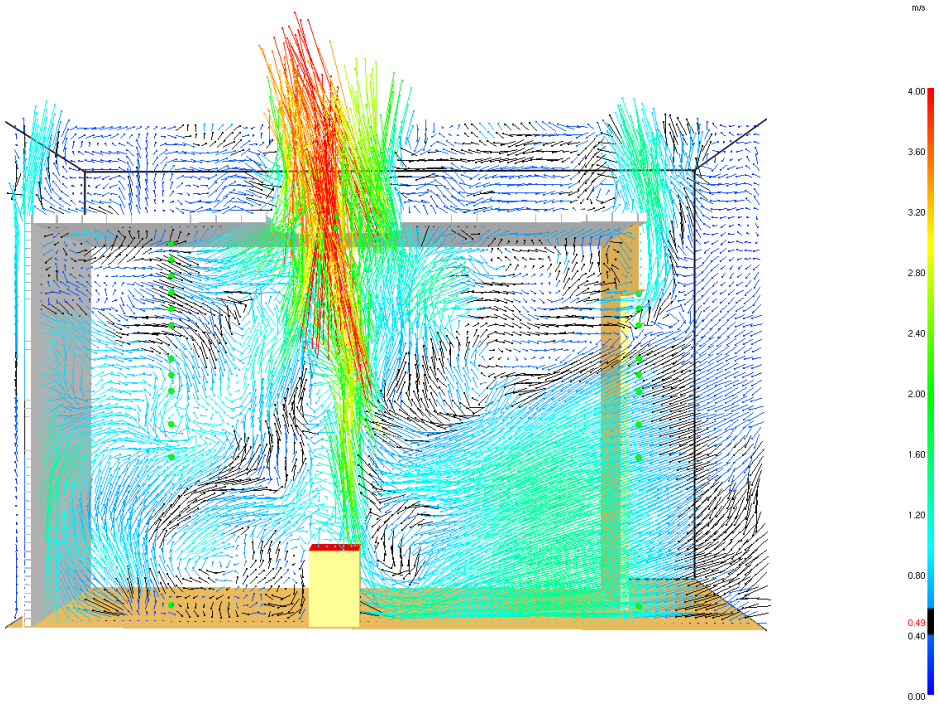

Figure 27. Test 8, after 1500 seconds, hole, 5 cm grid size. The effect of air entrainment on the plume. Red indicates a air velocity of 4 m/s.

6.3 Comparison between Pyrolysis Models

The two pyrolysis models has been compared with the experimental tests. The output parameters time to hole, temperature and hole size has been compared with the same parameters measured in the experimental tests. The most agreeable values has been selected. See comparisons on temperature in figure 28 and figure 29. See comparisons on hole size and time to hole in table 5 and table 6 below.

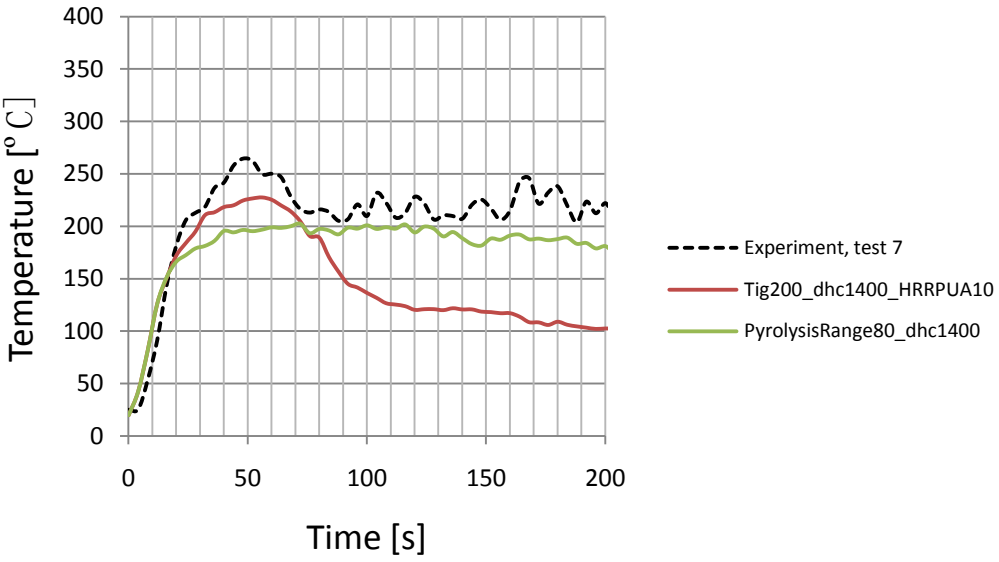

Figure 28. Temperature profile for test 7 showing the best result from pyrolysis model I and II at height 2,3 m. The red line shows pyrolysis model I and the green pyrolysis model II.

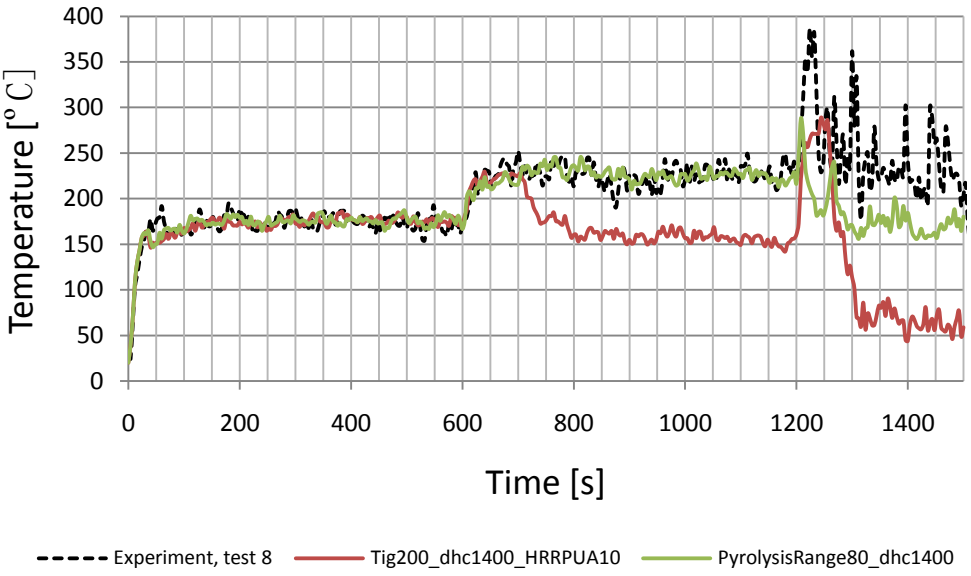

Figure 29. Temperature profile for test 8 showing the best result from pyrolysis model I and II at height 2,3 m. The red line shows pyrolysis model I and the green pyrolysis model II.

Table 5. Pyrolysis model I Vs. Pyrolysis model II.

Test 7		
	Time to hole [s]	**Hole size [m]**
Experiment, test 7	50	0,65 x 0,65
Tig200_dhc1400_HRRPUA10 (P I)	54,6	0,65 x 0,55
PyrolysisRange80_dhc1400 (P II)	15,6	0,35 x 0,35

Table 6. Pyrolysis model I Vs. Pyrolysis model II.

Test 8		
	Time to hole [s]	**Hole size [m]**
Experiment, test 8	1228	0,95 x 1
Tig200_dhc1400_HRRPUA10 (P I)	690,8	ca 2 x 2
PyrolysisRange80_dhc1400 (P II)	1205,3	0,75 x 0,65

6.4 Simulations of complex geometries

Textiles are used in complex buildings therefore it is also important to be able to use the burn away option in more complex geometries as compared to the ISO room. An attempt to use the model was thus made on two of the complex geometries used in Contex-T.

For both geometries pyrolysis model I has been used. Listed in Table 7 below are the used parameter values.

Table 7. Input parameters for simulation of complex geometries, VUB and Wagner building, model I, 20 cm grid size.

Test	**VUB & Wagner**
Parameter	
Density [kg/ m^3]	1300
Thickness [mm]	0,5
Conductivity [W/m·K]	0,23
Specific Heat , Cp[kJ/kg.K]	0,97
HRRPUA [kW/m^2]	10
Heat of Combustion, ΔH_c [kJ/kg]	3000
Radiative fraction	0,35
Ignition Temperature [°C]	150
Bulk density	0,21
Burner output [MW]	1
HRRPUA, burner [kW/m^2]	1000
Burner area [m^2]	1
Burner height [m]	0,5

The FDS file for the complex geometries VUB and Wagner was created by importing an AutoCAD DXF file in Pyrosim where the correct parameters was given. The AutoCAD DXF files was provided by SP (26). The geometry was then exported as an FDS file. Small changes was finally made manually before the actual simulation. The input file for the VUB-building is about 7500 command lines and 11400 command lines for the Wagner building. Because of the magnitude none of these input files was included in this document.

6.4.1 The VUB building

The measures of the VUB building are roughly 8,5 m in diameter at base and 4,3 m high. Two grid sizes has been simulated, 20 and 10 cm. Grid independence has not been reached, see further discussion in chapter 8.3. The process of creating and simulating is shown in Figure 30 through Figure 34 below.

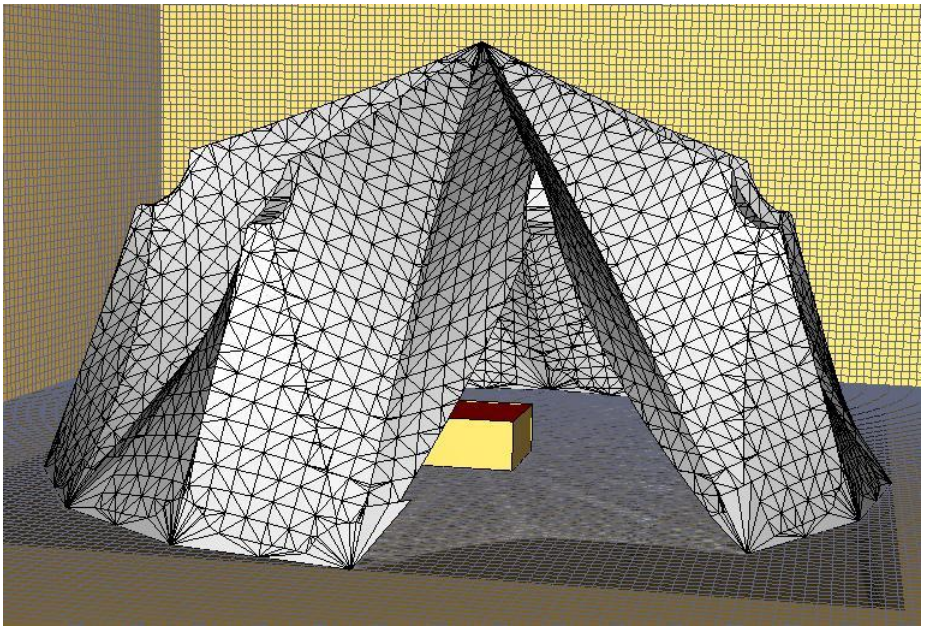

Figure 30. The VUB building in Pyrosim before creating the mesh.

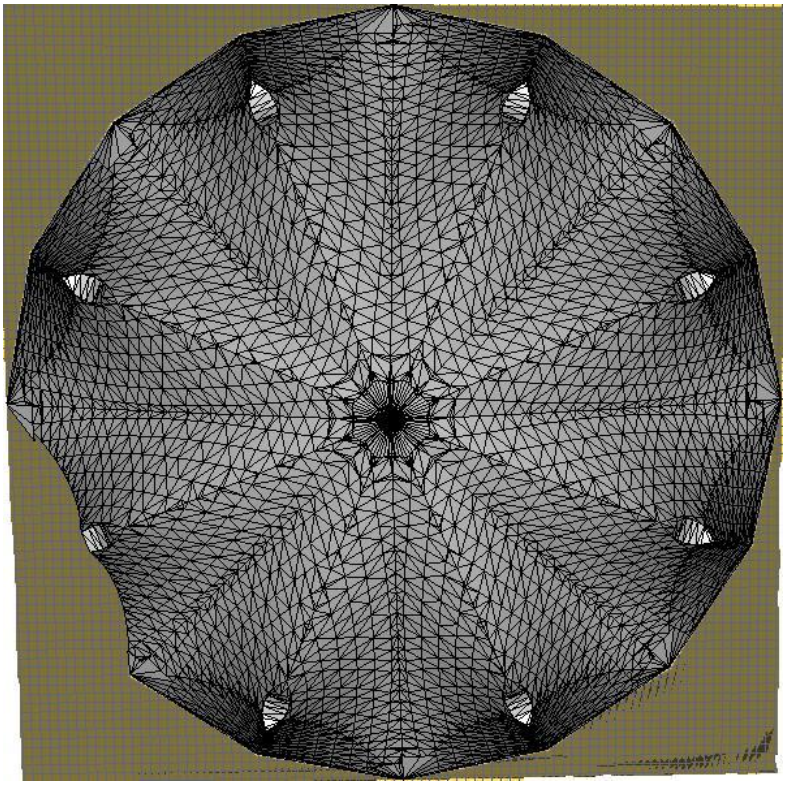

Figure 31. The VUB building in Pyrosim before creating the mesh, seen from above.

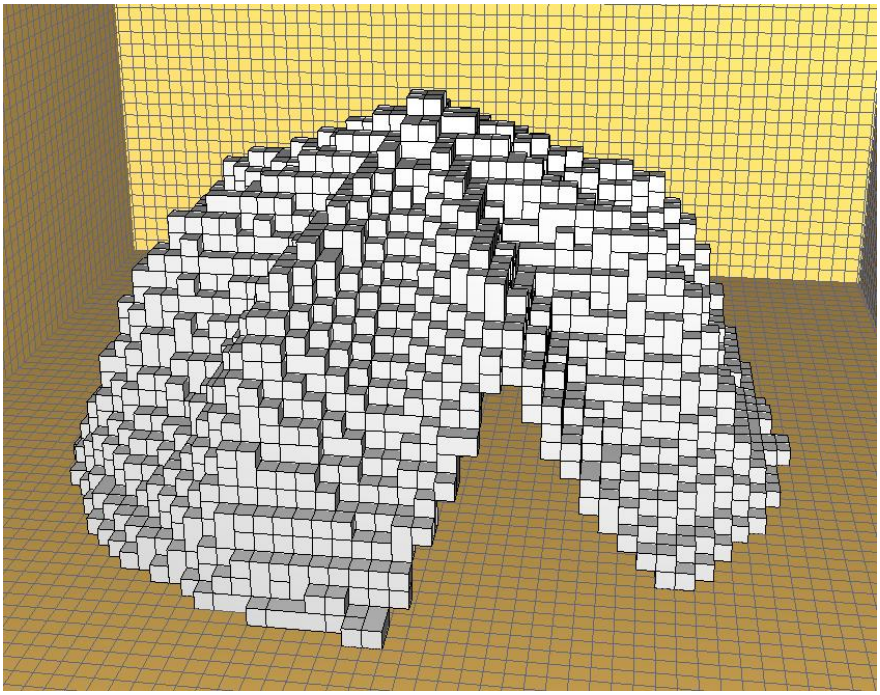

Figure 32. The VUB building in Pyrosim with 20 cm grid size.

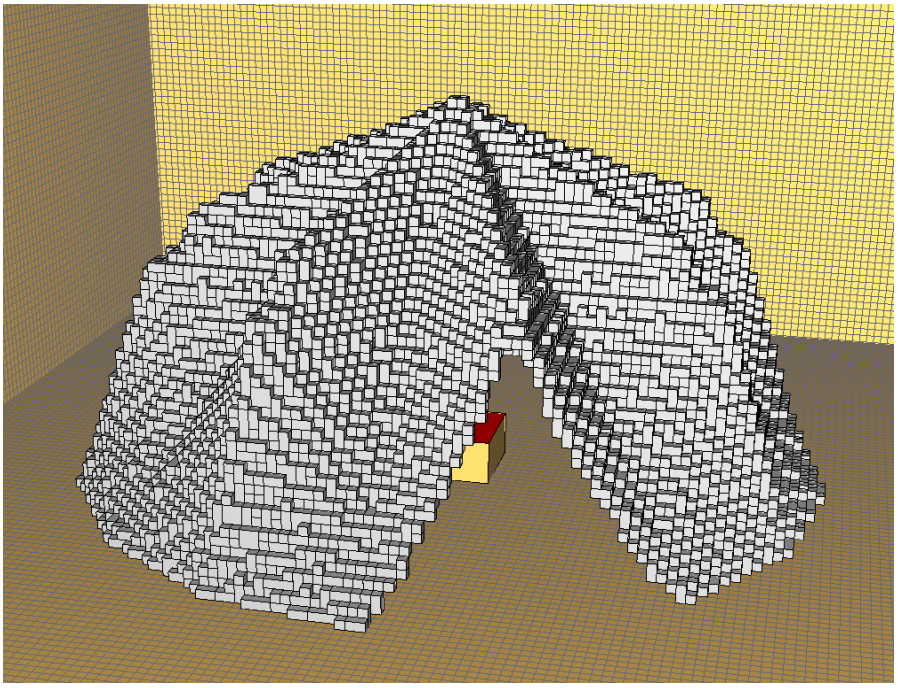

Figure 33. The VUB building in Pyrosim with 10 cm grid size.

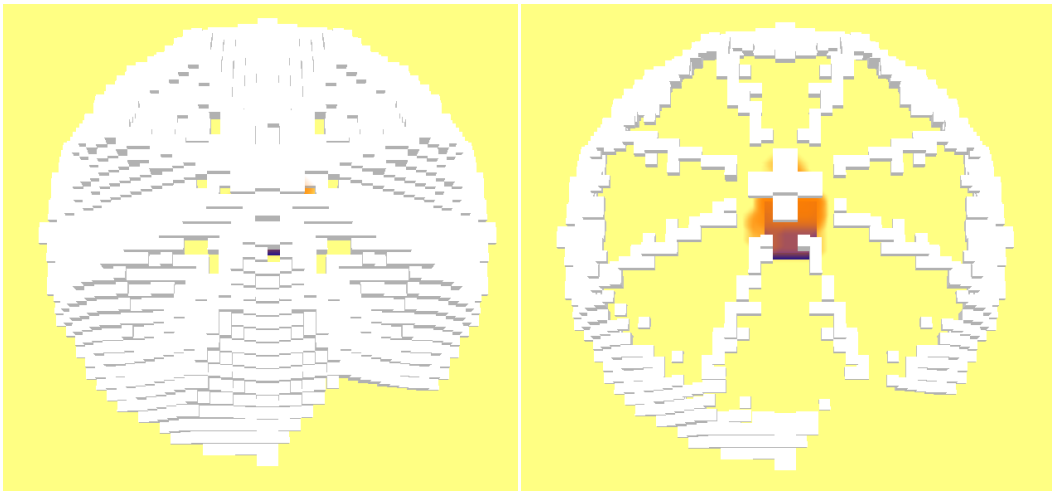

Figure 34. The VUB building, 20 cm grid size. Coarse grid results in problems with accurately simulating burn away.

6.4.2 The Wagner building

The measures of the Wagner building are 14,4 by 12 m and 4 m high. Two grid sizes has been simulated, 20 and 10 cm. Grid independence has not been reached, see further discussion in chapter 8.3. The process of creating and simulating is shown in Figure 35 through Figure 39 below.

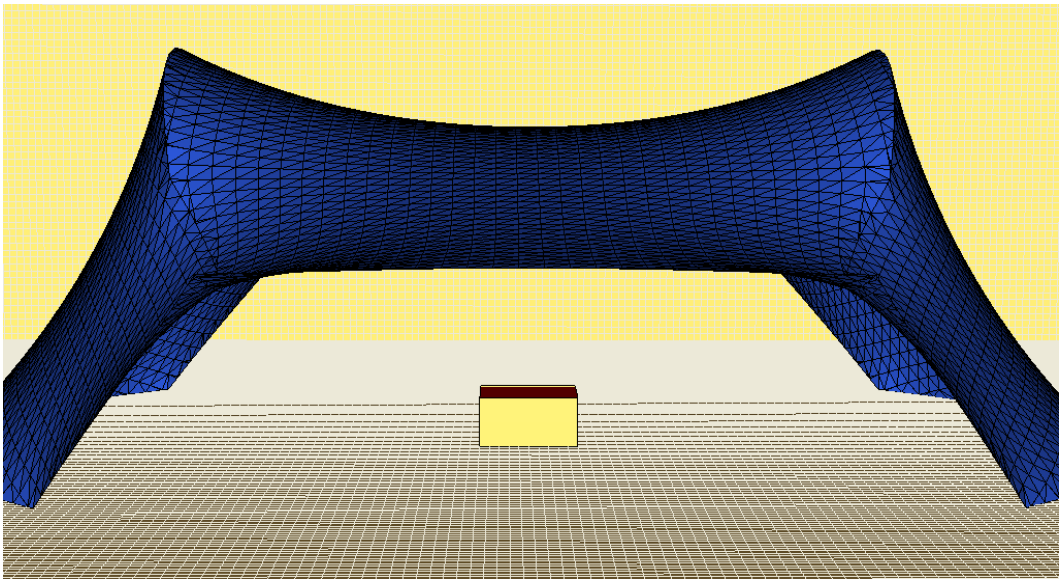

Figure 35. The Wagner building in Pyrosim before creating the mesh.

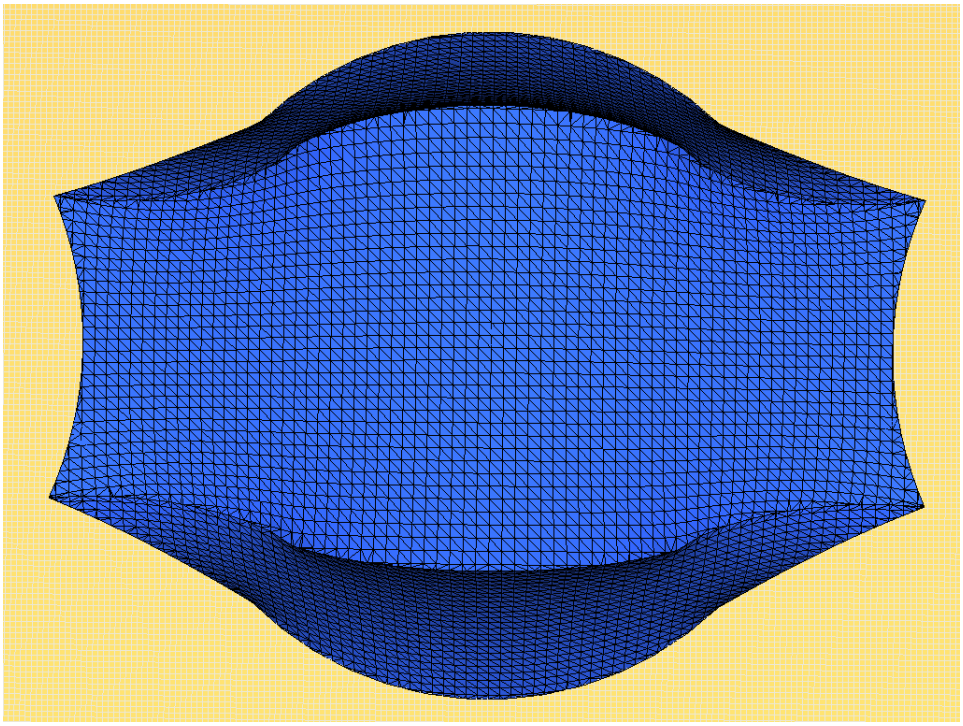

Figure 36. The Wagner building in Pyrosim before creating the mesh, seen from above.

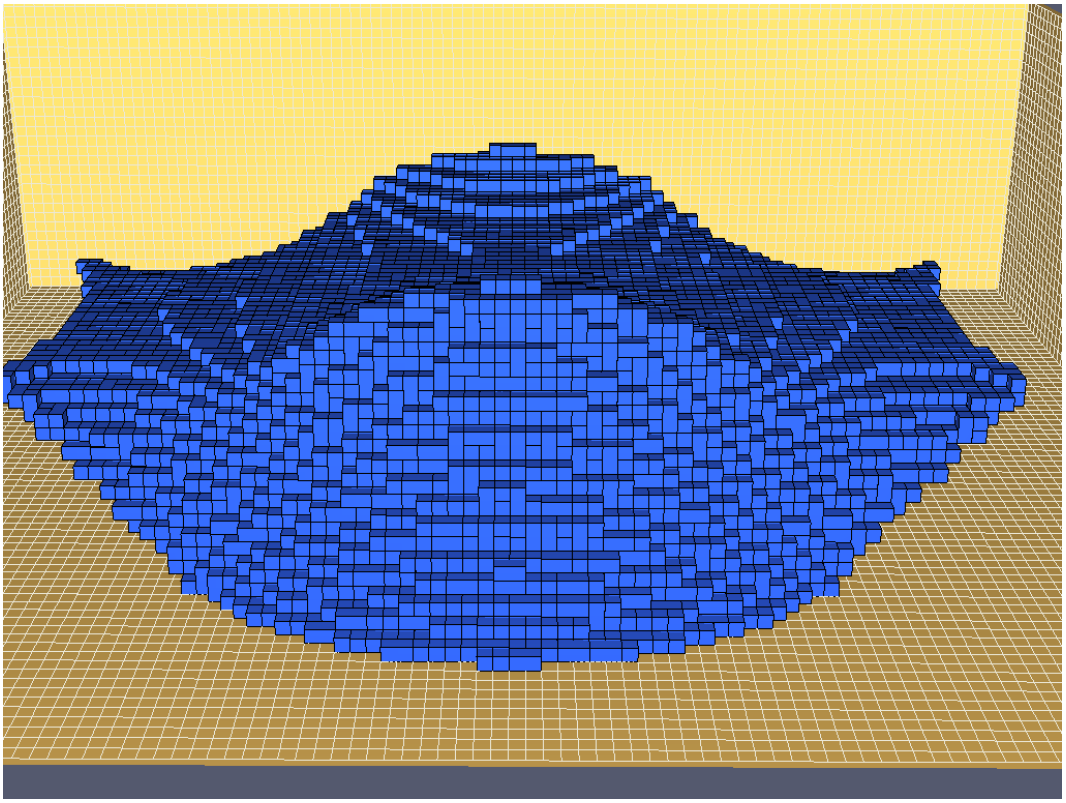

Figure 37. The Wagner building in Pyrosim with 20 cm grid size.

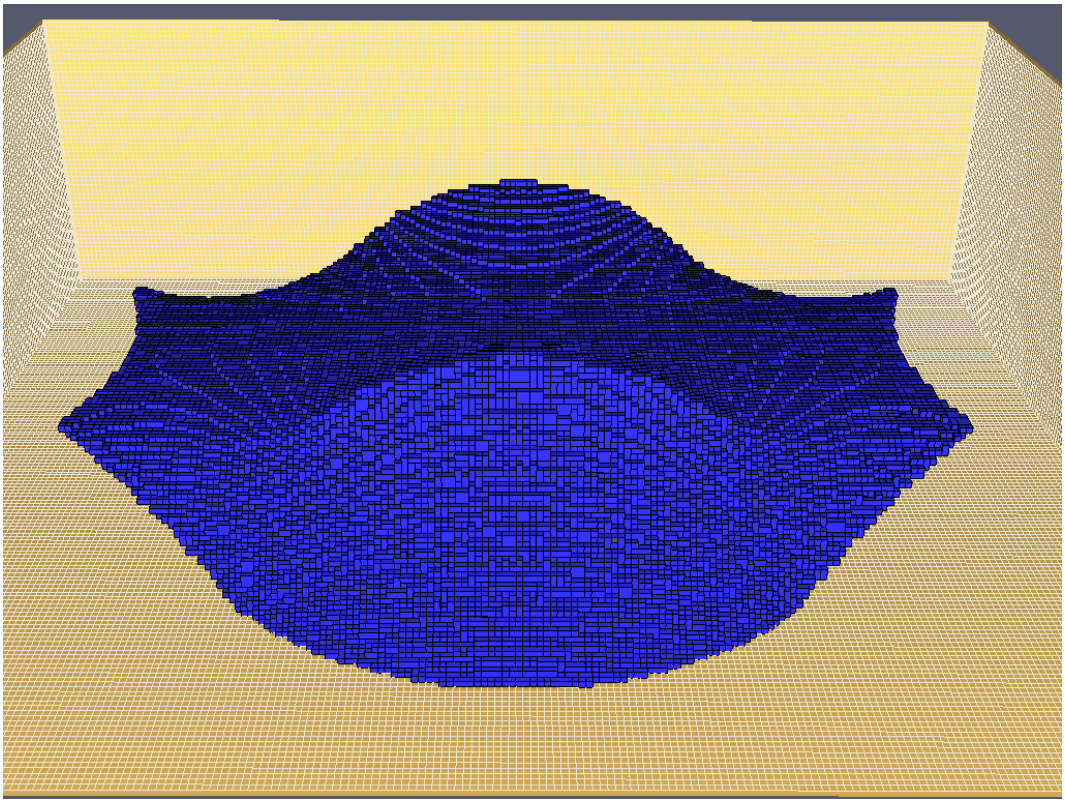

Figure 38. The Wagner building in Pyrosim with 10 cm grid size.

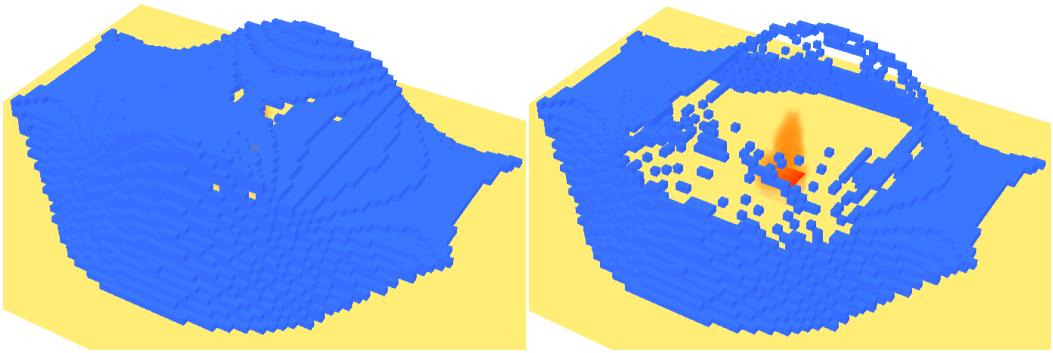

Figure 39. The Wagner building, 20 cm grid size. Coarse grid results in problems with accurately simulating burn away.

7 Uncertainties and errors

CFD programs like FDS are simulation programs which purpose is to mimic the real world of physics with mathematics. It is obvious that this is a massive undertaking which cannot be accomplished without a certain degree of simplification. Consequently simulations rarely match physical observations exactly (27). Divergence arise due to uncertainty and error, which are separated in computational engineering as two independent concepts.

In CFD, deficiency due to uncertainty is often associated with modelling in preference to the discretization (turning continuous models and equations into discrete counterparts). According to (27) the definition of uncertainty in the CFD field is: 'A potential deficiency in any phase or activity of the modelling process that is due to the lack of knowledge'. Consequently, uncertainty is very hard to quantify because one can only speculate about the magnitude or even if the deficiency exists at all. Unless and only if new information is gathered and learned or if external help is acquired can uncertainty be quantified.

General uncertainties for CFD are modelling errors like the simplification of physical models, coefficients used are not fully known or simply that the physics behind are not understood.

Errors on the other hand are defined as: 'A recognizable deficiency in any phase or activity of modelling and simulation that is not due to lack of knowledge'. Unlike uncertainties, errors are usually easier to identify. Because the knowledge is already present the identification of errors are usually solved by performing control procedures. Furthermore errors can be divided into two separate categories, acknowledged errors and unacknowledged errors. (27)

Acknowledged errors are those deficiencies that are recognized by the analyst. In other words they can be described as either unavoidable or intentionally introduced to make a problem manageable. Consequently the analyst is more or less aware of them, thus when introduced into the modelling or simulation process they are already quantified to some extent. Examples of acknowledged errors include simplifying assumptions, finite precision calculations and conversion of partial differential equations into discrete numerical equations. (28)

Unacknowledged errors occurs due to blunders or mistakes such as input data errors, programming mistakes and problems with compiler optimization or language libraries. This type of error is not recognized by the analyst/user, however they are not unrecognizable. Unfortunately unacknowledged errors are not easy to approximate, constrain or arrange, simply because there are no straightforward methods. One might detect these errors just by doing a double-check, or in some cases, like in FDS, the program will to some extent inform when a mistake has been made, or with external help thanks to redundancy in the procedures connected to the analysis. (28)

Verification and validation are processes and tools with which one can quantify uncertainty and errors. These processes also provides credibility and confidence in both the computational tool and the user. Hence Rubini (27) argues that verification and validation is the most important part of the CFD process.

Verification deals with the mathematics of the problem and not the physics. In other words, making sure the equations are solved correctly. According to Rubini (27) the

definition of verification is: ' The process of determining that a model implementation accurately represents the developer's conceptual description of the model and the solution to the model'. Code verification and solution verification are the two categories into which verification can be divided.

Code verification focuses on error evaluation which in turn intends to identify usage errors and programming/implementation errors or the like. Verification of this type could be an examination of the source code. Solution verification on the other hand is all about error estimation, which purpose is to quantify convergence errors and truncation errors. Verifying grid convergence i.e. grid independence belongs to this category. (27)

Validation is defined as 'The process of determining the degree to which a model is an accurate representation of the real world from the perspective of the intended uses of the model' (27). In contrast to verification, validation intends to analyze whether the correct equations were solved. Validating a simulation is done by comparing it to experimental measurements. However, experimental results are not in any way absolute, but hold their own uncertainties and errors. Thus these are also discussed.

7.1 Specific uncertainties and errors

The sources of uncertainties and errors can be divided into three parts; the first part has to do with the validation experiments, the second with the compilation of the input parameters and the third has to do with modelling and simulation. See further discussion under chapter 1.

7.1.1 Validation experiments

All of the validation experiments has been performed by SP. It is therefore difficult for the authors to be speak in detail concerning uncertainties and errors for these experiments. Uncertainties and errors identified by the authors are presented below.

It is important to note that only one of each validation experiment has been conducted. The experimental times and temperatures that is constantly referred to and compared against are therefore not secured. If they were to be conducted again all of the results would be different to some extent. It is therefore not meaningful to compare result down to solitary seconds and degrees. Additionally unacknowledged errors due to human error might have been made, compromising the validity of the experiments, which could have been eliminated by doing second tests.

Acknowledged errors include the proportion between the design fire and the size of the building is not realistic, especially concerning which type of building textile membranes are meant for. More on this is discussed in chapter 1. Another acknowledged error is the sudden increase of the burner output, which does not represent a true scenario. For example, this error give rise to the apparent threshold values seen in Table 13. Furthermore the recorded time to hole for the different experiments was done manually i.e. visual estimation. There are of course a number of unacknowledged errors, which has not been accounted for by the authors.

7.1.2 Input parameters

As mentioned in 5.1, the burn away model is a coarse simplification of the very complicated combustion process. In a real fire, a hole can arise from a number of reasons or a combination of some, such as pyrolysation or burning off, but also

melting of the material or because of local weaknesses in the material. The burn away option does not account for the latter two. To achieve realistic results the simulation with the burn away option should rely on correct input parameter values. These are however not easy to find or determine. For instance, there is a considerable margin of error in choosing the pyrolysis range from a TGA result, see Figure 40 and Figure 41 in Appendix B – TGA results, as well as in the results from the cone calorimeter and TPS. The statistic foundation is not sufficient when only one or a pair of tests has been conducted, especially when the few that has been performed differ relatively much. This was the case when determining heat of combustion from the results given by the cone calorimeter, thereof the broad interval in which this parameter has been varied (see Appendix E – Variation of parameters). Consequently, the result of the tests give an interval for each parameter. In combination with several other parameters with the same prerequisites it is often difficult to mimic the real scenario. As a consequence the margin of error in each of the input parameters results in a great margin of error in the output. Beyler, Craig et al (10) argues that TGA may not be suitable to use for quantifying fire performance. Their main problems has to do with the low heating rate, the small amount of material and the lack of heat feedback. The TGA made on the materials in this thesis used a heating rate of 5K/minute while 10-100K/s are common under fire conditions. These low TGA heating rates may draw attention to kinetics not important at the real fire heating rates (10).

The cone calorimeter (23) has been used to establish values for ignition temperature, heat of combustion and heat release rate per unit area. Although the cone calorimeter is a widely used test tool it has flaws. Enright and Fleischmann (29) demonstrates that the uncertainty is very high when testing low heat release rates. They argue that the assumption of combustion expansion and uncertainties in measuring the oxygen concentrations significantly contributes to the uncertainty. They further suggests a number of improvements with the test method. A number of years has passed since the study was published in 1999 but the authors of this thesis has not been able to establish if these improvements has been implemented in the ISO standardized test method. However, a number of articles published after the latest modification of the ISO-test in 2002 refer to Enright's and Fleischmann's article. E.g. Lukošius and Vekteris (30)refers to the former article and interpret the results meaning that the relative uncertainty with HRRPUA greater than 50 kW/m^2 have an uncertainty of ±5 % to ±10 %. Furthermore at heat release and volume flow rates representative for room fire experiments, Yeager (31) found that the relative uncertainties varied from ±5 % to ±11 % depending on which physical unit the test seeks.

Radiative fraction and heat of reaction was determined by literature study. As mentioned in chapter 5.3 radiative fraction was chosen for propane and has not been adjusted to fit the textile membrane. This is an acknowledged error due to the fact that FDS only allows for one fuel. The determination of the parameter heat of reaction is an acknowledged error, which has been calculated based on several assumptions. An extensive discussion in chapter 8.2 has been written on the subject.

To conclude, there are uncertainties in finding the correct input data, especially determining the heat of combustion from the cone calorimeter tests and the width of the pyrolysis range from the thermo gravimetric analyser. When using a wide possible range of several parameters, where most are sensitive to change, it becomes more difficult to find the true input and successfully emulate the validation experiments.

7.1.3 Simulation and modelling

When creating an input file for FDS, two user related errors can occur; either acknowledged errors or unacknowledged errors. The first has been handled to some degree due to the fact that many of the input parameters has been established in tests and the authors are aware of the weaknesses of these tests. The variation of the parameters is an example of this. The second one however, which includes errors due to miscalculations and other mistakes, is harder to quantify. Double checks has been made to reduce such errors.

The thermocouples placed directly on the membrane, under and above the ceiling may be influenced by conduction of heat through the material that FDS cannot account for. The mounting of a thermocouple directly on a material cannot be exactly simulated in FDS. The wall temperature device in FDS simulates the real measured value better than the thermocouple device does. This is also affected by the fact that FDS cannot account for the melting of the material but in reality the melting will affect the output of the thermocouple.

During the validation experiments pieces of the membrane was seen to fall down and molten membrane was seen to drip from the roof. This indicates that the hole growth is not only dependent on the burning away of the membrane. The melting point has probably a considerable effect on the hole opening but this cannot be accounted for with the burn away option. This option can only simulate the pyrolysation of the material but not the complex reactions leading up to the starting of this process, see chapter 3.1.

The simulated materials are built up of two kinds of polyester threads, one lengthways and one edgeways, coated in polyvinyl chloride, PVC. These two threads probably has different strength, sustainability and melting point. When heated the membrane will at first give away plasticizers. Then the PVC will break down when chlorine leaves in the form of hydrogen chloride. This makes the material weaker and indicates that linear strain is important for hole formation. As mentioned in the former paragraph, processes before actual ignition effects the evolution of holes. These are effects that has not been and cannot be simulated in FDS.

SP has shown differences in CPU time for the same simulation on different computers. This is not a problem the authors has observed but the computer systems has only been compared for test 7. Maybe this variations does not occur until after long CPU times. The creators of FDS argue that the variations occurs because of the random number generator, RND (32).

Lindström and Lund (5) has used a very simple geometry where they vary chosen input parameters with Monte Carlo simulations, within a set interval. They then investigate the variation's impact on a chosen output parameter, visibility. The goal is to visualize the problems with picking a static value to represent a whole range of likely values for a certain input parameter. They found, that out of three varied input parameters one had a small effect, one a moderate effect and one did greatly affect the output parameter. When these where all varied the influence on the output was even greater. The simulations performed in Lindström and Lund's thesis are much less complex when it comes to the number of parameters used, compared to the current thesis. Values for heat of combustion, ignition temperature, radiative fraction, pyrolysis range and residue has been distributed into intervals and therefore varied. Other parameters have been set to constants using test values, but may not be considered absolute, i.e. holding uncertainties. Specific to this thesis are:

reference temperature, conductivity and specific heat. Lindström and Lund show that even in less complex scenarios, varying a limited number of parameters can have a great effect in the results. The current thesis deals with a more complex scenario with more parameters to consider. Thus the uncertainties in the results become even greater.

Studies have shown that the use of material parameters derived from small-scale tests does not give a perfect flame spread in FDS (6). This might indicate that material parameters from small-scale tests does not describe material parameters in full-scale satisfyingly (6). Staffansson (6) argues that for his simulations with flame spread the material properties has a low impact on the simulation results compared to the faults caused by FDS modelling of the physical processes. These are; heat transfer from gas to material, external radiation from flames and fire gases and transport of fire gases.

8 Discussion

In the following chapter the conditions, assumptions and results of the simulations are discussed. The chapter is divided between the different pyrolysis models and the complex geometries. The first part is however devoted to general discussions.

An important goal with our part in the Contex-T project is to investigate if hole burning in the membrane will work as a natural smoke ventilator, improving the conditions for evacuating people. This makes the design of the validation experiments questionable. To begin with, tests are not in actual size and shape. Secondly and more important the positioning and heat release rate relative the room size is over proportioned, especially when considering the timescale when evacuation is supposed to take place. It is not likely that a flame will reach the membrane ceiling in a real fire, considering the large building constructions planned. As can be seen in Figure 48 and Figure 49 there is a great difference between test 7 and 8. In test 7 the flame immediately reaches the ceiling while in test 8 the flame does not reach the ceiling until after the last burner output increase at 1200 s. This makes test 8 more applicable to real fire scenarios, especially if fire safety is taken to account. In larger buildings, like full-scale VUB or Wagner, with textile membranes and with lots of people the initial fire process is most important. Results show that in most cases no hole will arise in the membrane until the flame reaches it. This essentially means that the evacuation conditions in the building will have reached critical levels long before smoke evacuation has begun. This is a reason why results from test 8 and 10 are more important than test 7 and 9.

When regarding time to hole and hole size the first conclusion drawn when reviewing the results is that pyrolysis model I seems to agree best with experimental tests 7 and 9 while pyrolysis model II shows the best results for tests 8 and 10. The temperature agreement is generally somewhat better with model II, especially for test 8 and 10. While it for the temperatures in test 7 and 9 depends on what time span one is interested in. Pyrolysis model I shows the temperature rise better while pyrolysis model II shows a better agreement throughout the whole simulation. See comparisons on temperature in figure 28 and figure 29. See comparison on hole size and time to hole in table 5 and table 6.

The burn away option must be improved, especially when it comes to the parameter bulk density. It is unclear exactly how FDS calculates for this parameter, the source code was unfortunately never studied due to time shortage. However several simulations concludes that bulk density might not be eligible for these experiments. This includes phase changes and the fact that the equation contradicts itself. When a higher heat of combustion is chosen the mass of the membrane is increased, which in turn increases time to hole, see Table 8. Also as long as the geometry does not consist of straight angles bulk density will be useless. The reasoning above is valid for all simulations using bulk density.

For simulations with CFD codes grid independency is important to reach to avoid numerical errors (33). Two grid sizes has been simulated for all geometries, see Appendix E – Variation of parameters but grid independency has not been ensured. An example supporting this statement is the difference in mean temperature of the flame. The temperature is much lower with coarser grid while the finer grid will produce a higher flame with increased mean temperature, see Figure 13 through Figure 18 and Figure 23 and Figure 24. The ceiling temperature is about 250 degrees higher with the finer grid just before hole opens up. The difference is not as big when comparing the simulated membrane temperature, because of the thermal

inertia of the membrane. The size of this error depends on the so called characteristic diameter of the fire. It is shown in Appendix C – Characteristic diameter of the fire that for the coarse grid this diameter has a lower value than is recommended. What this means is that the resolution of the fire is too poor to accurately simulate the flame and plume. For the simulations showed in Figure 14 and Figure 15 the first cells in the ceiling reaches temperature of ignition after 16,5 s (5 cm grid) and 166,5 s (10 cm grid). Studying time to hole in Table 9 one can draw the conclusion that the time to burn off one cell is virtually the same regardless of grid size. The time to burn off being the time from which the cell reaches the temperature of ignition until the cell is removed from the domain. The reasoning above is a very good example of how better resolution leads to higher temperatures.

Although grid independence has not been reached grid sizes under five cm has not been simulated. Such simulations would render a too long simulation time and in some cases would contain too many cells for the computers to handle. To solve this problem multiple meshes could be introduced but in these small geometries that would mean a considerably poorer quality of the results.

8.1 Pyrolysis model I

This chapter focuses on the function and results of pyrolysis model I. The results are found in chapter 6.2 and Table 8 through Table 11 in Appendix E – Variation of parameters.

There is a significant difference between the size of the two holes in the case with temperature of ignition 150ºC and 200ºC, see Figure 11 and Figure 12. The hole size is therefore dependent of the temperature of ignition. Figure 12 shows that the hole does not grow to its final size until the burner output increase after 300 s. This is because the static burner rate correlates to the door opening which creates a steady state where only the centre of the plume produce a high enough temperature for ignition. When burner output increases so does the temperature of the plume, which ignite a larger area of the ceiling. In practice this means a larger amount of cells will reach the critical ignition temperature of 200ºC, because a greater volume of the plume will reach this temperature.

When comparing simulations in Figure 12 it is clear that ignition temperature has a considerable influence on the scenario. For the lower temperature of ignition (150ºC) the temperature of the smoke layer accelerates when the roof is ignited instead of decreasing with the venting out of hot gases. The reason for this is probably that when the roof is ignited energy from the combustion contributes to the heating of the unburned ceiling. This phenomenon does not have the same influence with the higher temperature of ignition (200ºC) because a considerable lesser amount of cells will reach this temperature. The loss of hot gases through the door has a greater influence in the later case. Because heat of vaporization is not used there is no coupling between burn rate and heating of the material (7). The energy needed to gasify the material is disregarded which lead to a faster than realistic heating of the smoke layer and material.

For the simulations showed in Figure 14 and Figure 15 the first cells in the ceiling reaches temperature of ignition after 16,5 s (5 cm grid) and 166,5 s (10 cm grid). Studying time to hole in Table 9 one can draw the conclusion that the time to burn off one cell is virtually the same regardless of grid size. The time to burn off being the time from which the cell reaches the temperature of ignition until the cell is removed from the domain. This is a very good example of how better solution leads

to higher temperatures. The burning off, of one cell takes approximately 32 s for the thickness 0,5 mm and bulk density 0,11 in test 7. This account for at least the simulations with ignition temperature 150, 160, 180 and 190ºC and the simulation with 10 cm grid. This shows that the HRRPUA works as a ON button when the cells temperature reaches the set ignition temperature. When the burning has started it does not stop or slow down even if the temperature should dip under the ignition temperature. The size and shape of the hole is greatly influenced by variations of ignition temperature and/or the bulk density. An example is illustrated in Figure 50 and Figure 51 where the combination of a low positioning of the burner and a high bulk density leads to the burning off of the whole roof. The figures show that all cells which has been in contact with the hot smoke layer is burned off. The flame does not reach the ceiling and therefore ignition temperature is not reached early, as in simulations 7 and 9. In turn the temperature in the smoke layer builds up homogenously. When the burner output is increased the ignition temperature is reached above the flame. But because the bulk density is high the burning off of cells take a long time. This allows the whole smoke layer to reach ignition temperature before a hole appears big enough to prevent the temperature of the smoke layer from reaching the ignition temperature.

Furthermore pyrolysis model I only allows for one ignition temperature. Plastics however does not have a set ignition temperature but decomposes and combusts in several stages, see chapter 3.1. See also discussion under 8.2 below. To conclude, pyrolysis model I simplifies the process a great deal.

8.2 Pyrolysis model II

This chapter focuses on the function and results of pyrolysis model I. The results are found in chapter 6.2 and Table 12 through
Table 15 in Appendix E – Variation of parameters.

As the information in the FDS User Guide on this model is poor some tests were conducted. Among other things results have shown that the membrane temperature does not have to reach the reference temperature for a hole to develop. See Figure 46 and Figure 47 in Appendix F – Additional . Another test was aimed at straightening out the connection between residue and time to hole. As can be seen in Table 12 (rows 3, 10 and 11) the time to hole increases with increased fraction of residue. It is not clear why this happens. The reason might be what the FDS User Guide describes ”The mass of the object is based on the densities of the all material components (MATL), but it is only consumed by mass fluxes of the known species. If the sum of the gaseous yields (Section 11.2.3) is less than one, it will take longer to consume the mass.” (7) Once again, the User Guide is not very detailed.

The use of residue (see Table 12 –
Table 15) does not generally seem to influence the time to hole with simulations with five cm grid size, only the growth of the hole is influenced. The influence is more apparent with the coarser ten cm grid where both the time to hole and the growth of the hole is influenced. When studying equation 8.6 in the FDS User Guide (7) it is obvious that the introduction of residue reduces the peak reaction rate slightly. This decrease in energy released from the burning of the membrane does not influence the finer grids as much as the coarser because the mean temperature is considerably higher with the finer grid. The influence of residue is also noticeable with a wider pyrolysis range. The same reasoning is probably valid here. A wider pyrolysis range leads to combustion taking off at lower temperatures. For test 8 the flame does not immediately reach the ceiling and will therefore heat up slowly, thus

undergo combustion during a longer time with a high pyrolysis range compared to a low pyrolysis range. In other words the reaction rate during the steady state between the effect increase at 600 and 1200 s is considerably higher in the case with higher pyrolysis range since the pyrolysis process starts 40ºC earlier than with the lower pyrolysis range. For test 7, on the contrary, the flame does reach the ceiling raising the temperature of the ceiling cells very fast. When temperature raises fast the 40ºC difference will have a smaller effect since the combustion will start at nearly the same time. The critical effect between pyrolysis ranges for this scenario will therefore be the difference in acceleration of the reaction rate, which is much higher for the lower pyrolysis range.

Heat of reaction is a parameter associated to pyrolysis model II. No extensive testing has been performed on this parameter because of shortage of time and due to the uncertainties concerning the definition of the parameter. The user guide (7)defines the heat of reaction as the amount of energy consumed per unit mass of reactant that is converted into something else i.e. the enthalpy difference between the products and the reactant. If heat of reaction is given a positive value energy is taken out of the system, endothermic reaction. The Technical Reference Guide (34) mentions heat of reaction very briefly and does not really explain how the value should be chosen. Verification of the equations in the Technical Reference Guide in purpose of understanding the parameter's relation to the pyrolysis process in detail has not been made. In the discussion group site for FDS and Smokeview (35) the topic concerning heat of reaction is frequently discussed. After extensive review of the threads it is still uncertain what heat of reaction is and especially for plastics. One possible conclusion is that heat of reaction is the required energy for all sub step reactions until the production of all the volatiles which will undergo pyrolysis. The heat of reaction could in this case be equivalent to heat of gasification. Values for PVC and Polyester are found in SFPE (36) and Drysdale (13). However other inquires on the discussion group suggests that heat of reaction is only one part of heat of gasification, namely the conversion phase onto another solid or fuel gas. The heating of the material from ambient temperature till the conversion occurs is left out in the heat of reaction parameter. Due to the complicated process of decomposition and combustion of plastics, see chapter 3.1, it is all but impossible to select a specific value for heat of reaction. Typically the phase change of a substance consumes a lot more energy than the heating (specific heat), why heat of gasification should give a reasonably accurate value with a known overestimate (37). Finally one suggestion for heat of reaction for polymers is the so called heat of decomposition obtained by differential scanning calorimetry. The mechanism is not clear yet, but in general the heat of decomposition is the consequence of several processes, such as bond dissociation, new bond formation, and volatile evaporation (38). Se Appendix E – Variation of parameters for used values and results.

In test 8 only twelve seconds differ between time to hole with 10 respectively 5 cm grid size. As can be seen in Figure 24 the flame is much hotter with finer grid but the flames influence on the ceiling is not as great in test 8 as in test 7. The characteristic fire diameter is within recommended values with the finer grid. Therefore the mean temperature which is calculated for each cell is more realistic with the finer the grid. In test 8 with finer grid the temperature of the ceiling is greater to start with but after about 20 s the smoke layer's thickness has reached the door and isolates the ceiling from the otherwise relatively large heating effect of the flame and plume. At this time the pressure and temperature differences between inside and outside are large, thereby increasing turbulence, see Figure 25. Air turnover is about the same for respectively grid size but there are more eddies in the finer grid. The plume's effect on the ceiling is decreased because of the turbulence cooling effect on the

plume, which makes the heat from the flame and plume spread more evenly in the smoke layer. This is why there is no great difference in time to hole between the grid sizes for test 8. This should be compared to test 7 that is much more sensitive for changes in grid size. The reason is simple, in test 7 the flame and plume has a more direct contact with the ceiling because the burner is 0,55 m closer to the ceiling. Therefore the flame and plume temperature difference between the two grid sizes has a greater influence on the ceiling than in test 8. The higher positioning of the burner also means that air can be mixed in with the plume efficiently from the bottom without affecting it to the extent as in test 8 where the air mixes in more from the side, see Figure 25 - Figure 27. Consequently a higher positioning of the burner leads to a more stable flame.

Figure 19 and figure 18 shows that pyrolysis model II does not agree with experimental values for tests 7 and 9. The common denominator is that these are the tests with the highest placed burner.

Pyrolysis model II with the Arrhenius type of reaction rate seems to have a better potential to simulate the experimental results than model I with the prescribed burn rate. The Arrhenius function represents pyrolysation as function of temperature derived from an actual experimental TGA test. Looking at these tests, see Appendix B – TGA results, with pyrolysis model I in mind, it is but a huge simplification in choosing a specific value for ignition temperature as of which a constant rate of reaction must be chosen. If a low ignition temperature is chosen, the peak reaction rate cannot be chosen, thus severely overestimating the rate of pyrolysation and in turn underestimating time to hole. Choosing a higher ignition temperature to correlate for this error can have great consequences, compare rows two and three in Table 9. Raising the ignition temperature with only 10ºC prolongs time to hole with amazingly 560 seconds due to the set threshold value determined by the steady state phenomena. If there was not an increase in burner effect after 600 seconds a hole would never have opened up. Consequently pyrolysis model I is not eligible for complex pyrolysation like textile membranes coated with two types of plastics.

8.3 Complex geometries

It has been shown that it is possible to import complex geometries(see chapter 6.4) into FDS via Pyrosim. It has not been shown that the burning away and opening of holes can be simulated correctly. There is a need for finer grids when working with complex geometries. However the CPU time was ten days for one of the used geometries simulated on one of today's fastest personal computers. The cluster Lunarc (see Appendix A) could not simulate this geometry at all because of insufficient memory.

The complex geometry is like any other geometry in FDS, an approximation where the building is simplified to fit a Cartesian grid. In this case the grid sizes 20 and 10 cm has been used. This leads to more serious faults in the rendering of a given geometry as it grows more complex. In the case with the VUB building this becomes obvious. Perfectly vertical and horizontal materials is rendered with a thickness of one cell. However, most parts of this geometry slopes/tilts in at least one dimension. This means that the walls in many places are two, three or even four cells thick. This problem is most obvious around the beams, or rather where the beams would be in the real geometry. Great angles arise near the beams and to emulate this with cubes results in several cubes overlapping each other. As a result the hole formation (burn away) becomes unrealistic. This happens because heat transfer is partially blocked and also because more mass must burn away, due to overlapping since one cell is

configured to represent the thickness and mass of the membrane. This is probably the reason for the results shown in, Figure 34 and Figure 39. To solve this, one must find a way to substitute BULK_DENSITY to achieve a homogenous layer or be able to simulate with a much finer grid. Unfortunately it would probably have to be DNS (Direct Numerical Simulation) quality.

9 Conclusions

Results show that it is possible to use the burn away option in FDS to model the opening up of a hole in textile membranes. The quality of the results compared to the validation experiments has varied for the pyrolysis models and the different tests. No simulations has perfectly mimicked the validation experiments and in a lot of cases the difference has been extensive. Great precaution should be taken when using the burn away option for fire safety design purposes.

The feature of a hole opening in a textile membrane due to burning away is considered important for fire safety design of buildings with these membranes. From the results of this study the conclusion can be drawn that an opening for such a purpose will not occur until the flame reaches the ceiling. When the hole reaches a size that will evacuate a considerable amount of smoke the conditions in the room are not acceptable for personnel evacuation. In other words: using textile membrane as a fire safety precaution for natural smoke evacuation is not reasonable.

Pyrolysis model II with the Arrhenius type of reaction rate seems to have a better potential to simulate the experimental results than model I with the prescribed burn rate.

There are uncertainties in finding the correct input data, especially determining the heat of combustion from the cone calorimeter tests and the width of the pyrolysis range from the thermo gravimetric analyser. When using a wide possible range of several parameters, where most are sensitive to change, it becomes more difficult to find the true input and successfully emulate the validation experiments.

Finally the report shows that it is possible to import complex geometries to FDS and use the burn away option as well. However the fact that only Cartesian coordinates are allowed in FDS is a huge problem. At the moment this makes it impossible to accurately simulate complex geometries for fire safety design purposes.

10 Further studies

- There is room for improvement concerning determination of ΔH_c in the cone calorimeter. Several layers of the material could perhaps be placed on top of each other and thus decrease the uncertainty.

- The results from the TGA differed noticeably. Initially the results were above 300 ºC and in the later test only 280 ºC. A greater number of tests would lessen the uncertainty. It would also be interesting to study how the temperature slope in the TGA influence the result.

- Although the parameter was not judged to influence the results noticeably in this study, it is recommended to include heat of vaporization (HEAT_OF_VAPORIZATION) when using model I in the future.

- Further studies are needed to straighten out how residue works in pyrolysis model II.

- Work with pyrolysis model II started late and it has not been studied to the same extent as pyrolysis model I. It might be interesting to study it further.

- To acquire satisfying results from simulations with the complex geometries a finer grid size is needed. Such a simulation will require a fast CPU and a substantial amount of random-access memory (RAM) to run efficiently. It would be wise to consider dividing such a room in several meshes to save calculation time.

11 References

1. **Andersson, Petra and Blomqvist, Per.** *Large-scale fire tests with textile membranes for building applications.* Borås : Sveriges tekniska Forskningsinstitut, 2010. SP Technical Note.

2. Contex-T. [Online] [Cited: 11 11 2010.] http://contex-t.ditf-denkendorf.de/index.php?option=com_rsgallery2&page=inline&gid=7&limit=1&Itemid=49&limitstart=35.

3. Contex-T. [Online] [Cited: 11 11 2010.] http://contex-t.ditf-denkendorf.de/index.php?option=com_rsgallery2&page=inline&gid=7&limit=1&Itemid=49&limitstart=7.

4. Contex-T. [Online] [Cited: 11 11 2010.] http://contex-t.ditf-denkendorf.de/index.php?option=com_rsgallery2&page=inline&gid=7&limit=1&Itemid=49&limitstart=6.

5. **Lindström, Tor and Lund, David.** *A method of quantifying user uncertainty in FDS by using Monte Carlo analysis.* Lund : Department of Fire Safety Engineering and Systems Safety, Lund University, 2009.

6. **Staffansson, Leif.** *Flame spread modeling in FDS5 – determination of input parameters and evaluation at different scales.* Lund : Department of Fire Safety Engineering and Systems Safety, Lund University, 2009.

7. **McGrattan, Kevin, et al.** *Fire Dynamics Simulator (Version 5) User's Guide.* Maryland : NIST Special Publication 1019-5, NIST Building and Fire Research Laboratory, 2010.

8. **Platt, David K.** *Engineering and High Performance Plastics Market Report.* s.l. : Rapra Technology Limited, 2003.

9. **Zhang, Huiqing.** *Fire-safe Polymers and Polymer Composites.* Amhurst, Massachusetts : Polymer Science and Engineering, University of Massachusetts, 2004.

10. **Beyler, Craig L and Hirschler, Marcelo M.** Section 1, Chapter 7 - Thermal Decomposition of Polymers. *SFPE Handbook of Fire Protection Engineering - Third edition.* Quincy, Massachusetts : National Fire Protection Association, 2002.

11. **Troitzsch, Jürgen.** *Plastics Flammability Handbook - Principles, Regulations, Testing, and Approval - Third Edition.* München : s.n., 2004.

12. **Harper, Charles A.** *Handbook of Building Materials for Fire Protection.* Lutherville, Maryland : Technology Seminars Inc., 2004.

13. **Drysdale, Dougal.** *An introdution to Fire Dynamics, Second Edition.* s.l. : John Wiley & Sons, 2005.

14. BBR 5:513 Surface finishes and claddings in certain premises (BFS 2002:19). *Boverket's Building Regulations.* 2002.

15. **Blomqvist, Per and Hjohlman, Maria.** *Fire tests with textile membranes on the market - results and method development of cone calorimeter and SBI test methods.* Borås : SP Technical Research Institute of Sweden, 2010. SP Report 2010:23.

16. BBR 5:11 Alternative design (BFS 1995:17). *Boverket's Building Regulations.* 2002.

17. **Blomqvist, Per.** *Ph.D. Senior Research Scientist.* 4 11 2010.

18. **Bengtsson, Staffan, et al.** *Brandskyddshandboken. Rapport 3134.* Lund : Department of Fire Safety Engineering and Systems Safety, Lund University, 2005.

19. BBR 5:51 Requirements regarding materials, surface finishes and claddings. *Boverket's Building Regulations.* 2002.

20. **Burström, Per Gunnar.** *Byggnadsmaterial - Uppbyggnad, tillverkning och egenskaper.* Lund : Studentlitteratur, 2001.

21. **Andersson, Petra and Blomqvist, Per.** *D3.3.a Performance based fire safety engineering – full scale tests (WP3 Task 3.3.2).* Borås : SP Technical Research Institute of Sweden, Fire Technology, 2009.

22. Pyrosim. *Thunderhead Engineering.* [Online] Thunderhead Engineering, 28 5 2010. [Cited: 28 5 2010.] http://www.thunderheadeng.com/pyrosim.

23. *ISO 5660-1, Reaction-to-fire tests – Heat release, smoke production and mass loss rate- Part 1: Heat Release rate (cone calorimeter method).* Geneva : International Organization for Standardization, 2002.

24. *ISO 22007-2 Plastics -- Determination of thermal conductivity and thermal diffusivity -- Part 2: Transient plane heat source (hot disc) method.* Geneva : International Organization for Standardization, 2008.

25. **Beyler, Craig L.** Section 3, Chapter 11, Fire Hazard Calculations for Large, Open Hydrocarbon Fires. *SFPE Handbook of Fire Protection Engineering - Third edition.* Quincy, Massachusetts : National Fire Protection Association, 2002.

26. **Andersson, Petra.** Scientist. 2010.

27. **Rubini, Philip A.** *CFD 2010.* Lund : Lund University, 2010.

28. **Oberkampf, William L, et al.** Error and uncertainty in modeling and simulation. *Reliability Engineering and System Safety.* 2001, Vol. 75.

29. *Uncertainty of Heat Release Rate Calculation of the IS05660-4 Cone Calorimeter Standard Test Method.* **Patrick, Enright A and Flesichmann, Charles M.** Christchurch : Fire Technology, 1999, Vol. 35.

30. *Precision of Heat Release Rate Measurement Results.* **Lukošius, A and Vekteris, V.** Vilnius : Measurement Science Review, 2009, Vol. 3.

31. *Uncertainty Analysis of Energy Release Rate Measurement for Room Fires.* **Yeager, Raymond W.** s.l. : Journal of Fire Sciences, 1986, Vol. 4, pp. 276-296.

32. **McGrattan, Kevin.** *Mathematician, NIST Building and Fire Research Laboratory.* 2009.

33. **Phil, Rubini.** CFD questions. s.l. : School of Engineering, Cranfield University, England, 2008.

34. **McGrattan, Kevin, et al.** *Fire Dynamics Simulator (Version 5) Technical Reference Guide Volume 1: Mathematical Model.* Baltimore, Maryland : NIST, 2010.

35. **NIST Building and Fire Research Laboratory.** *FDS and Smokeview Discussions.* [Online] [Cited: 10 10 2010.] http://groups.google.com/group/fds-smv.

36. **Tewarson, Archibald.** Section 3, Chapter 4, Generation of Heat and Chemical Compounds in Fires. *SFPE Handbook of Fire Protection Engineering - Third edition.* Quincy, Massachusetts : National Fire Protection Association, 2002.

37. **Jones, Loretta and Atkins, Peter.** *Chemistry: Molecules, Matter and Change, Fourth Edition.* s.l. : W. H. Freeman, 2000.

38. *Fire-Safe Polymers and Polymer Composites.* s.l. : U.S Department of Transportation Federal Aviation Administration, 2004.

39. **Linné, Mark.** *Tabellsamling Brandkemi (VBR 022).* Lund : Department of Fire Safety Engineering and Systems Safety, Lund University, 2005.

40. *Verification and Validation of Selected Fire Models for Nuclear Power Plant Applications, Volume 2: Experimental Uncertainty.* Rockville, Maryland, Palo Alto, California : U.S. Nuclear Regulatory Commission, Office of Nuclear Regulatory Research (RES), Electric Power Research Institute (EPRI), 2007.

Appendix A – System specifications

System 1, Lunarc (Cluster owned by Lund University)
CPU 2 Xeon 5160 (3.0 GHz, dual core)
Memory 4 Gb (1 Gb per core)
Linux distribution CentOS 5.3 x86_64 (RHEL4 compatible)

System 2, Private (Personal computer, Andreas Lennqvist)
CPU 4 IntelCore i7 920 (2.67 GHz, quad core)
Memory 6 Gb
Windows Vista Ultimate (64-bit)

System 3, Private (Personal computer, Joel Andersson)
CPU 2 IntelCore Duo T8300 (2.4 GHz, dual core)
Memory 2 Gb
Windows Vista HomeBasic (32-bit)

Appendix B – TGA results

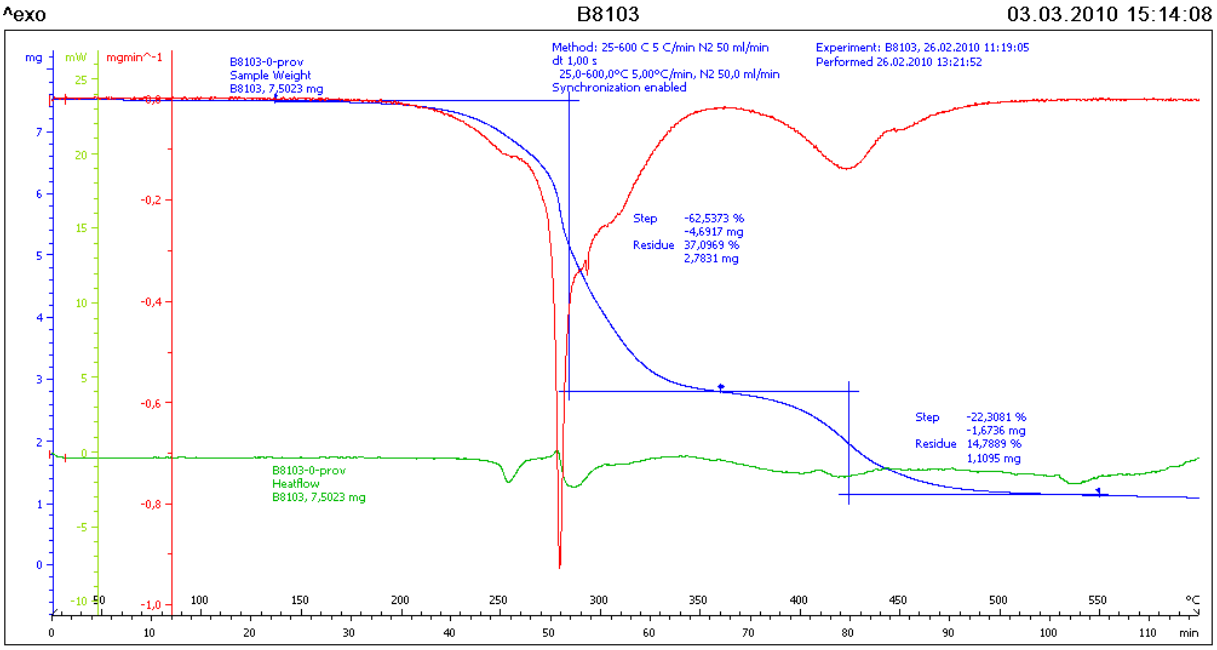

Figure 40. Results from thermo gravimetric analysis of the thin membrane (test 7 and 8). The blue line represents the sample weight, the red represents the weight loss per time and the green the heat flow .

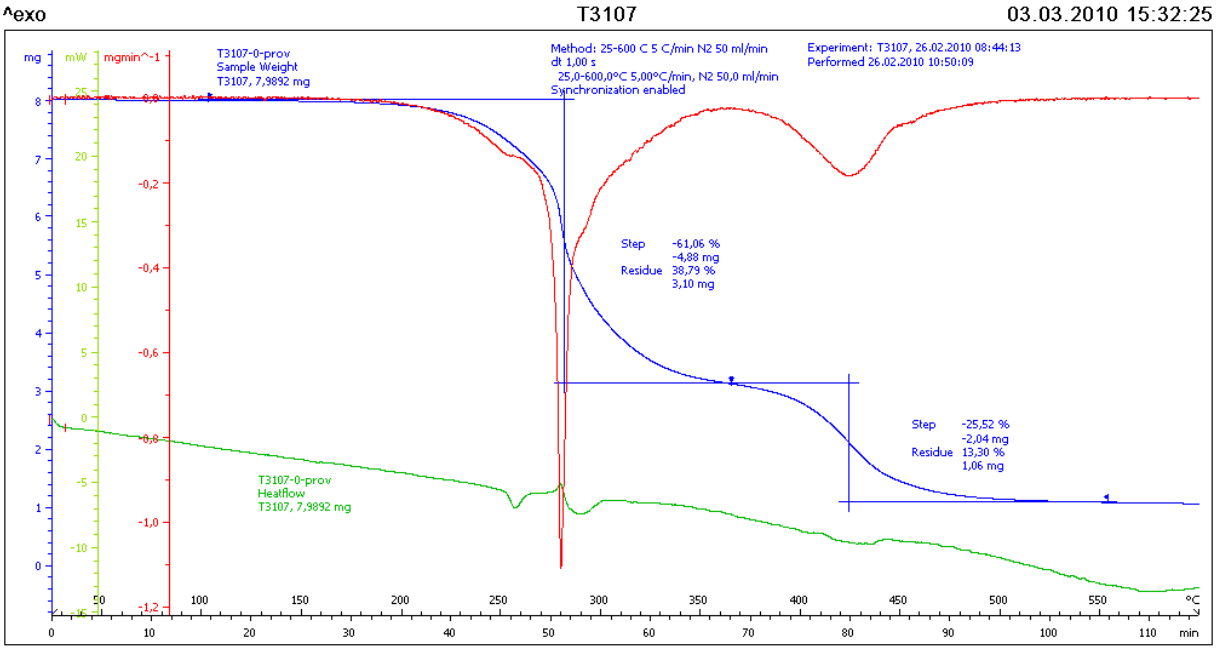

Figure 41. Results from thermo gravimetric analysis of the thicker membrane (test 9 and 10). The blue line represents the sample weight, the red represents the weight loss per time and the green the heat flow .

Appendix C – Characteristic diameter of the fire

Mesh dimensions – characteristic diameter of the fire:
Equation 6.1 in the FDS User Guide (7),

$$D^* = \left(\frac{\dot{Q}}{\rho_\infty c_P T_\infty \sqrt{g}}\right)^{\frac{2}{5}} = \left(\frac{(0{,}3 * 0{,}3) * 1556 * 0{,}68}{1.1 \cdot 1040 \cdot 291.5 \cdot \sqrt{9.81}}\right)^{\frac{2}{5}} = 0.372$$

Values for $\rho_\infty, c_P \; and \; T_\infty$ were taken from Linné (2005) (39) and the heat release rate was set to a constant value of 95 kW, to represent the average value of the fire growth during the time when holes appeared. The number of computational cells spanning the characteristic diameter is given by,

$$D^*/\delta x = 0.372/0.1 = 3{,}72$$

since the cell size is 0,1 meter. The value of 3,72 is not within the recommended values, 4-16, which are mentioned in the FDS User Guide (7) and in the NUREG report (2007). (40) This could explain the differences between the grid sizes, since a nominal cell size 0,05m would yield a value of 7,44 instead of 3,72.

Appendix D – Input file

This is an input file for test 8, model II that shows good results both concerning time to hole and temperature.

```
&HEAD CHID='Test8_ref280_range80_dhc1400'/
&TIME T_END=1500/
&DUMP RENDER_FILE='test8.ge1', NFRAMES=2000, WRITE_XYZ=.TRUE., DT_DEVC=4./

&MESH ID='MESH', IJK=60,90,60, XB=-0.2000,2.80,0.00,4.50,0.00,3.00/

&MISC  BNDF_DEFAULT=.FALSE. /

&MATL ID='PVC',
    SPECIFIC_HEAT=0.97,
    CONDUCTIVITY=0.23,
    DENSITY=1300
    REFERENCE_TEMPERATURE=280.,
    PYROLYSIS_RANGE=80.,
    N_REACTIONS=1,
    NU_FUEL=1/

&SURF ID='PVC-SHEET-A',
    MATL_ID='PVC',
    COLOR='GRAY 80',
    BURN_AWAY=.TRUE.,
    BACKING='EXPOSED',
    THICKNESS=5.0e-004/

&MATL ID='UNBURNABLE',
    SPECIFIC_HEAT=1.,
    CONDUCTIVITY=0.1,
    DENSITY=600/

&SURF ID='UNBURNABLE-BOARD',
    MATL_ID='UNBURNABLE',
    BACKING='EXPOSED',
    THICKNESS=0.07/

&SURF ID='FIRE',
    COLOR='RED',
    HRRPUA=3333.,
    RAMP_Q='FIRE_RAMP_Q'/
&RAMP ID='FIRE_RAMP_Q', T=0.00, F=0.317/
&RAMP ID='FIRE_RAMP_Q', T=600.00, F=0.317/
&RAMP ID='FIRE_RAMP_Q', T=601.00, F=0.467/
&RAMP ID='FIRE_RAMP_Q', T=1200.00, F=0.467/
&RAMP ID='FIRE_RAMP_Q', T=1201.00, F=1.0/
&RAMP ID='FIRE_RAMP_Q', T=1500.00, F=1.0/

&DEVC ID='Door 0.1m', QUANTITY='THERMOCOUPLE', XYZ=1.20,0.71,0.10/
&DEVC ID='Door 1.0m', QUANTITY='THERMOCOUPLE', XYZ=1.20,0.71,1.00/
&DEVC ID='Door 1.2m', QUANTITY='THERMOCOUPLE', XYZ=1.20,0.71,1.20/
&DEVC ID='Door 1.4m', QUANTITY='THERMOCOUPLE', XYZ=1.20,0.71,1.40/
&DEVC ID='Door 1.5m', QUANTITY='THERMOCOUPLE', XYZ=1.20,0.71,1.50/
&DEVC ID='Door 1.6m', QUANTITY='THERMOCOUPLE', XYZ=1.20,0.71,1.60/
&DEVC ID='Door 1.8m', QUANTITY='THERMOCOUPLE', XYZ=1.20,0.71,1.80/
&DEVC ID='Door 1.9m', QUANTITY='THERMOCOUPLE', XYZ=1.20,0.71,1.90/
&DEVC ID='Door 2.0m', QUANTITY='THERMOCOUPLE', XYZ=1.20,0.71,1.99/
```

```
&DEVC ID='Room 0.1m', QUANTITY='THERMOCOUPLE', XYZ=1.20,3.55,0.10/
&DEVC ID='Room 1.0m', QUANTITY='THERMOCOUPLE', XYZ=1.20,3.55,1.00/
&DEVC ID='Room 1.2m', QUANTITY='THERMOCOUPLE', XYZ=1.20,3.55,1.20/
&DEVC ID='Room 1.4m', QUANTITY='THERMOCOUPLE', XYZ=1.20,3.55,1.40/
&DEVC ID='Room 1.5m', QUANTITY='THERMOCOUPLE', XYZ=1.20,3.55,1.50/
&DEVC ID='Room 1.6m', QUANTITY='THERMOCOUPLE', XYZ=1.20,3.55,1.60/
&DEVC ID='Room 1.8m', QUANTITY='THERMOCOUPLE', XYZ=1.20,3.55,1.80/
&DEVC ID='Room 1.9m', QUANTITY='THERMOCOUPLE', XYZ=1.20,3.55,1.90/
&DEVC ID='Room 2.0m', QUANTITY='THERMOCOUPLE', XYZ=1.20,3.55,2.00/
&DEVC ID='Room 2.1m', QUANTITY='THERMOCOUPLE', XYZ=1.20,3.55,2.10/
&DEVC ID='Room 2.2m', QUANTITY='THERMOCOUPLE', XYZ=1.20,3.55,2.20/
&DEVC ID='Room 2.3m', QUANTITY='THERMOCOUPLE', XYZ=1.20,3.55,2.30/

&DEVC ID='ceiling temp 2.39',QUANTITY='WALL_TEMPERATURE',XYZ=1.20,2.55,2.39,IOR=-
3/
&DEVC ID='roof temp 2.46',QUANTITY='WALL_TEMPERATURE',XYZ=1.20,2.55,2.46,IOR=3/

&DEVC ID='TC TAK 2.39',QUANTITY='THERMOCOUPLE',XYZ=1.20,2.55,2.39/
&DEVC ID='TC TAK 2.46',QUANTITY='THERMOCOUPLE',XYZ=1.20,2.55,2.46/

&DEVC ID='BURN RATE',QUANTITY='BURNING RATE',XYZ=1.20,2.55,2.39,IOR=-3/

&HOLE XB= 0.80,1.60, 0.69,0.76, 0.00,2.00/ Door

&OBST XB=-0.05,2.45, 0.70,0.75, 0.00,2.40, SURF_ID='UNBURNABLE-BOARD'/ Front wall
&OBST XB=-0.05,0.00, 0.75,4.35, 0.00,2.40, BULK_DENSITY=0.385, SURF_ID='PVC-SHEET-A'/
Left wall
&OBST XB= 2.40,2.45, 0.75,4.35, 0.00,2.40, BULK_DENSITY=0.385, SURF_ID='PVC-SHEET-A'/
Right wall
&OBST XB=-0.05,2.45, 4.35,4.40, 0.00,2.40, BULK_DENSITY=0.385, SURF_ID='PVC-SHEET-A'/
Back wall
&OBST XB=-0.05,2.45, 0.70,4.40, 2.40,2.45, BULK_DENSITY=0.385, SURF_ID='PVC-SHEET-
A',BNDF_OBST=.TRUE./ Ceiling
&OBST XB= 1.05,1.35, 2.40,2.70, 0.00,0.45, / Fire source
&VENT XB= 1.05,1.35, 2.40,2.70, 0.45,0.45, SURF_ID='FIRE'/ Fire source

&VENT SURF_ID='OPEN', XB=-0.2000,2.80,0.00,0.00,0.00,3.00, COLOR='INVISIBLE'/ Vent
&VENT SURF_ID='OPEN', XB=-0.2000,-0.2000,0.00,4.50,0.00,3.00, COLOR='INVISIBLE'/ Vent
&VENT SURF_ID='OPEN', XB=2.80,2.80,0.00,4.50,0.00,3.00, COLOR='INVISIBLE'/ Vent
&VENT SURF_ID='OPEN', XB=-0.2000,2.80,4.50,4.50,0.00,3.00, COLOR='INVISIBLE'/ Vent
&VENT SURF_ID='OPEN', XB=-0.2000,2.80,0.00,4.50,3.00,3.00, COLOR='INVISIBLE'/ Vent

&SLCF QUANTITY='VELOCITY', VECTOR=.TRUE., PBY=0.750/
&SLCF QUANTITY='VELOCITY', VECTOR=.TRUE., PBX=1.200/
&SLCF QUANTITY='VELOCITY', VECTOR=.TRUE., PBY=2.550/

&SLCF QUANTITY='TEMPERATURE', PBY=0.75/
&SLCF QUANTITY='TEMPERATURE', PBX=1.20/
&SLCF QUANTITY='TEMPERATURE', PBY=2.55/
&SLCF QUANTITY='TEMPERATURE', PBZ=2.35/

&BNDF QUANTITY='WALL_TEMPERATURE'/

&TAIL /
```

Appendix E – Variation of parameters

Here are selected parts of the output represented. The "Chart nr" column includes cross-references to charts showing that exact simulation in other parts of the report. The simulations marked pink are represented in figures in other parts of the report. Yellow indicates a varied parameter.

Pyrolysis model I

Table 8. Test 7. For all of these simulations time to hole in the experiment is 50 s, dimensions of the hole in the experiments is 0,65x0,65 m, thickness of the membrane is 0,5 mm, conductivity is 0,23 W/mK, specific heat 0,97 kJ/kgK and density 1300 kg/m^3.

Figure nr	ΔH_c [kJ/kg]	HRRPUA [kW/m^2]	TIG [ºC]	Bulk density	Radiative fraction	Grid size [mm]	Time to hole [s]	Hole size [m]	Comments
Figure 7, Figure 11	400	4	150	0,110	0,35	50	39,3	0.8x0.8	
	400	4	150	0,037	0,35	150	45,6	1 x 1	1
	1000	4	150	0,275	0,35	50	87,9	2,6x2,4 (hole in wall)	2
	3000	4	150	0,825	0,35	50	250,5	Whole roof and hole in wall	
Figure 7	6000	4	150	1,65	0,35	50	-		2
	400	2	150	0,11	0,35	50	71,7	2,1x1,5 (hole in wall)	2
	400	6	150	0,11	0,35	50	28,5	0,9x0,7	2
Figure 7	400	10	150	0,11	0,35	50	19,8	0,8x0,7	2
	400	14	150	0,11	0,35	50	16,2	0,8x0,75	2
	400	4	150	0,11	0,25	50	38,4	0,9x0,75	2
	400	4	150	0,11	0,3	50	38,4	0,95x0,8	2
	800	4	150	0,11	0,35	100	73,5		3
	400	4	150	0,055	0,35	100	40,8		4
Figure 7	1400	10	150	0,385	0,35	50	52,2	ca 2.4x2.4	5
Figure 7, Figure 12, Figure 28	1400	10	200	0,385	0,35	50	54,6	0,65x0,55	6

[1]Hole on the side wall after 360 s.

[2]Only simulated to 500 s.

[3] The purpose was to show that the formula for bulk density was correct. This should be compared to the first row. The only difference is the grid size (which gives twice the ΔH_c, because bulk density is the same as row one) which means that the ceiling is 10 cm thick and has twice the mass to burn away before hole opens. Time to hole is approximately doubled and this validates the formula. The small difference is probably caused by the temperature build-up which gives an increased pyrolysis.

[4] Grid independency , to be compared with first row, 1,5 s difference.
[5] Small openings on the side walls.
[6] A good example of the on/off function caused by the prescribed burn rate. Compare with the row above where a large part of the roof has reached ignition temperature before a hole is opened and hot gases is let out.

Table 9. Test 8. For all of these simulations time to hole in the experiment is 1228 s, dimensions of the hole in the experiments is 0,95x1 m, thickness of the membrane is 0,5 mm, conductivity is 0,23 W/mK, specific heat 0,97 kJ/kgK and density 1300 kg/m^3.

Figure nr	ΔH_c [kJ/kg]	HRRPUA [kW/m^2]	TIG [ºC]	Bulk density	Radiative fraction	Grid size [mm]	Time to hole [s]	Hole size [m]	Comments
Figure 8, Figure 14, Figure 16, Figure 18	400	4	150	0,110	0,35	50	51,8	ca 2,2 x 2,4	Extensive holes on both side walls
	400	4	170	0,110	0,35	50	90,8	ca 1,2 x 1,2	Extensive holes on both side walls
	400	4	180	0,110	0,35	50	651,8	ca 1,1 x 1,1	Extensive holes on both side walls
	400	4	230	0,110	0,35	50	813	1,6 x 1,75	
	400	6	150	0,110	0,35	50	41,3	1,3x2,4	Extensive holes on both side walls
Figure 8	400	10	150	0,110	0,35	50	32,3	2,4x2,4	Extensive holes on both side walls and the back wall
	400	12	150	0,110	0,35	50	30	2x2,4	Extensive holes on both side walls and the back wall
	400	4	150	0,110	0,3	50	50,3	2,4x2,4	Extensive holes on both side walls and small on back wall
	400	4	150	0,110	0,25	50	46,5	2x2	Extensive holes on both side walls
	1000	4	150	0,275	0,35	50	100,5	2,4x2,4	Extensive holes on both side walls and hole on the back wall
	2000	4	150	0,55	0,35	50	182,3	1,5x2,4	Extensive holes on both side walls and hole on the back wall
	4000	4	150	1,1	0,35	50	344,3	1,5x1x8	Small holes on both side walls
Figure 8, Figure 50, Figure 51	6000	4	150	1,65	0,35	50	507	Whole roof	Hole in ceiling and walls from lower part of the smoke layer and up. Small holes from radiation further down on the middle of side walls.
Figure 13, Figure 15, Figure17	400	4	150	0,055	0,35	100	205,5	ca 1,6 x 2,4	Extensive holes on both side walls
Figure 8	1400	10	150	0,385	0,35	50	65,3	ca 2,5 x 2,4	Extensive holes on both side walls
Figure 8, figur 29	1400	10	200	0,385	0,35	50	690,8	ca 2 x 2	Holes on both side walls

Table 10. Test 9. For all of these simulations time to hole in the experiment is 90 s, dimensions of the hole in the experiments is 0,63x0,62 m, thickness of the membrane is 1,1 mm, conductivity is 0,23 W/mK, specific heat 0,97 kJ/kgK and density 1045 kg/m^3.

Figure nr	ΔH_c [kJ/kg]	HRRPUA [kW/m^2]	TIG [ºC]	Bulk density	Radiative fraction	Grid size [mm]	Time to hole [s]	Hole size [m]	Comments
Figure 9	2100	10	150	1,021	0,35	50	130,8	The whole roof	Hole on great parts of the side walls.
Figure 9	2100	10	200	1,021	0,35	50	135,3	0,65 x 0,55	Evident result of the pyrolysis model's on/off function.

Table 11. Test 10. For all of these simulations time to hole in the experiment is 1235 s, dimensions of the hole in the experiments is 1,11 x 0,9 m, thickness of the membrane is 1,1 mm, conductivity is 0,23 W/mK, specific heat 0,97 kJ/kgK and density 1045 kg/m^3.

Figure nr	ΔH_c [kJ/kg]	HRRPUA [kW/m^2]	TIG [ºC]	Bulk density	Radiative fraction	Grid size [mm]	Time to hole [s]	Hole size [m]	Comments
Figure 10	2100	10	150	1,021	0,35	50	408,8	ca 2.4 x 2.4	Extensive holes on all three walls.
Figure 10	2100	10	200	1,021	0,35	50	756	The whole roof	Large holes on both side walls.

Pyrolysis model II

Table 12. Test 7. For all of these simulations time to hole in the experiment is 50 s, dimensions of the hole in the experiments is 0,65x0,65 m, thickness of the membrane is 0,5 mm, conductivity is 0,23 W/mK, specific heat 0,97 kJ/kgK and density 1300 kg/m^3. The reference temperature is 280°C.

Figure nr	ΔH_c [kJ/kg]	Pyrolysis range	Bulk density	Residue	Grid size [mm]	Time to hole [s]	Hole size [m]	Comments
	1000	160	0,137	N/A	100	27,9	0,60x0,50	
	2000	160	0,275	N/A	100	35,7	0,50x0,50	
Figure 23, Figure 24	3500	160	0,48	N/A	100	53,7	0,50x0,50	1
	4000	160	0,55	N/A	100	57,6	0,50x0,50	
	3500	80	0,48	N/A	100	28,5	0,40x0,40	
	3500	110	0,48	N/A	100	30,3	0,40x0,40	
	3500	240	0,48	N/A	100	69,3	0,60x0,50	
	3500	160	0,48	0,15 (residue density 5kg/m^3)	100	70,8	0,50x0,50	
	3500	160	0,48	0,15 (residue density 1300kg/m^3)	100	66,3	0,50x0,50	
	3500	160	0,48	Nu_fuel=0,3	100	120,9	0,30x0,30	
	3500	160	0,48	Nu_fuel=0,85	100	68,4	0,50x0,50	
	3500	160	0,48	N/A	100	355,5	0,20x0,20	1
Figure 19, Figure 23, Figure 24, Figure 25	3500	160	0,96	N/A	50	18,3	0,45x0,45	
Figure 19, Figure 28	1400	80	0,385	N/A	50	15,6	0,35x0,35	
Figure 19	1400	160	0,385	N/A	50	17,1	0,45x0,45	4
Figure 19	1400	80	0,385	Nu_fuel=0,85	50	15,6	0,35x0,35	
	1400	160	0,385	Nu_fuel=0,85	50	18	0,50x0,50	
	1400	160	0,385	N/A	50	20,4	0,45x0,45	2, 4
	1400	160	0,385	N/A	50	17,1	0,45x0,45	3, 4

[1] To be compared. The burner effect has in the later been lowered to 1000 kW/m^2. The flame does not reach the roof until after 301 s, i.e. after the first increase. If 300 s is subtracted from "time to hole" the difference between the simulations is only 1,8 s.
[2] In this simulation heat of reaction was included and set to 2500 kJ/kg.
[3] In this simulation heat of reaction was included and set to 200 kJ/kg.
[4] Compared to see influence of heat of reaction.

Table 13. Test 8. For all of these simulations time to hole in the experiment is 1228 s, dimensions of the hole in the experiments is 0,95 x 1 m, thickness of the membrane is 0,5 mm, conductivity is 0,23 W/mK, specific heat 0,97 kJ/kgK and density 1300 kg/m^3. The reference temperature is 280°C.

Figure nr	ΔH_c [kJ/kg	Pyrolysis range	Bulk density	Residue	Grid size [mm]	Time to hole [s]	Hole size [m]	Comments
	3000	160	0,825	N/A	50	984	0,75x0,80	
Figure 20, Figure 26, Figure 27	3500	160	0,962	N/A	50	996,8	0,75x0,80	1
	4000	160	1,100	N/A	50	1044	0,75x0,85	
	3500	120	0,962	N/A	50	1206,8	0,90x1	
	3500	200	0,962	N/A	50	774	0,80x0,80	Medium holes on side walls.
	3500	160	0,481	N/A	100	984,8		1
Figure 20, figure 29	1400	80	0,385	N/A	50	1205,3	0,75 x 0,65	2
Figure 20	1400	160	0,385	N/A	50	801	0,90 x 0,80	Hole on the sides. 2, 5
Figure 20	1400	80	0,385	Nu_fuel=0.85	50	1206	0,80 x 0,65	Only simulated to 1419 s.
	1400	160	0,385	Nu_fuel=0.85	50	894,8	0,80 x 0,85	Only simulated to 1441,5 s. Small holes on side walls.
	1400	160	0,385	N/A	50	800,3	0,9x0,8	Hole on the sides. 3, 5
	1400	160	0,385	N/A	50	759,8	0,9x0,8	Hole on the sides. 4, 5

[1] To be compared for grid independency.
[2] The reaction rate during the steady state between the effect increases at 600 and 1200 s is considerably higher in the case with pyrolysis range 160° C since the pyrolysis process starts 40° C earlier. With pyrolysis range 80° C the reaction rate is not sufficient for hole to open until after the 1200 s effect increase.
[3] In this simulation heat of reaction was included and set to 2500 kJ/kg
[4] In this simulation heat of reaction was included and set to 200 kJ/kg
[5] Compared to see influence of heat of reaction.

Table 14. Test 9. For all of these simulations time to hole in the experiment is 90 s, dimensions of the hole in the experiments is 0,63x0,62 m, thickness of the membrane is 1,1 mm, conductivity is 0,23 W/mK, specific heat 0,97 kJ/kgK and density 1045 kg/m3. The reference temperature is 280°C.

Figure nr	ΔH_c [kJ/kg]	Pyrolysis range	Bulk density	Residue	Grid size [mm]	Time to hole [s]	Hole size [m]
Figure 21	2100	80	1,02	N/A	50	24,3	0.40 x 0.40
Figure 21	2100	160	1,02	N/A	50	28,8	0.50 x 0.50
Figure 21	2100	80	1,02	Nu_fuel=0.85	50	24,9	0.35 x 0.40
	2100	160	1,02	Nu_fuel=0.85	50	30,6	0.50 x 0.50

Table 15. Test 10. For all of these simulations time to hole in the experiment is 1228 s, dimensions of the hole in the experiments is 1,1 x 0,9 m, thickness of the membrane is 1,1 mm, conductivity is 0,23 W/mK, specific heat 0,97 kJ/kgK and density 1045 kg/m3. The reference temperature is 280°C.

Figure nr	ΔH_c [kJ/kg]	Pyrolysis range	Bulk density	Residue	Grid size [mm]	Time to hole [s]	Hole size [m]	Kommentar
Figure 22	2100	80	1,021	N/A	50	1206	1 x 0,9	
Figure 22	2100	160	1,021	N/A	50	700,5	0,9 x 0,85	Large holes on side walls.
Figure 22	2100	80	1,021	Nu_fuel=0.85	50	1206	0,95 x 0,85	Only simulated to 1317 s.
	2100	160	1,021	Nu_fuel=0.85	50	873	0,8 x 0,75	Only simulated to 1405,5 s. Holes on side walls.

Appendix F – Additional graphs and slides

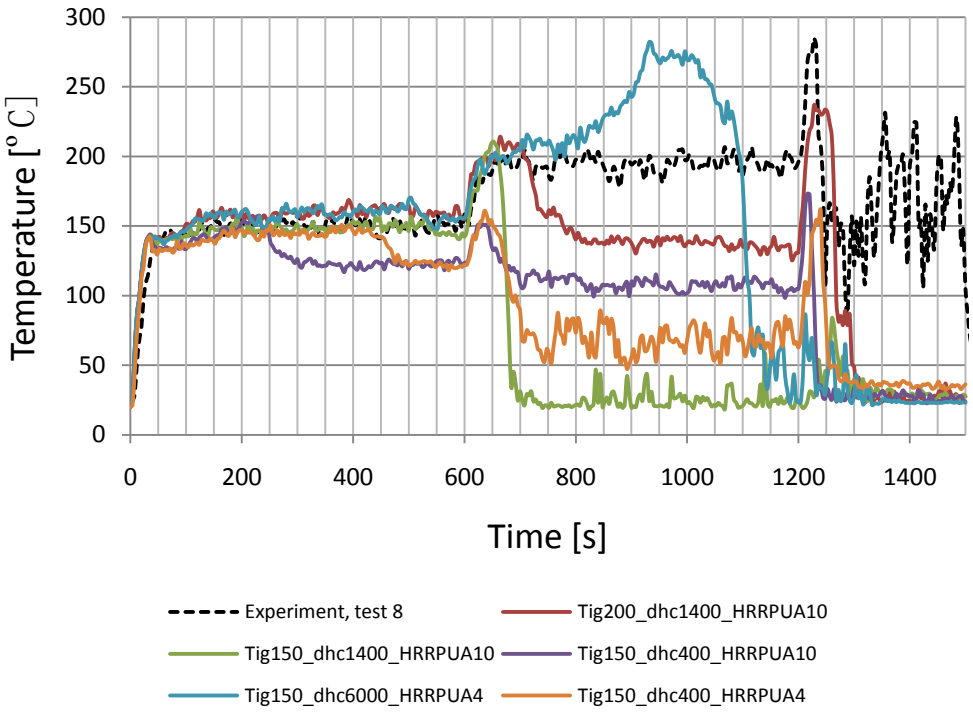

Figure 42. Model I, test 8. Thermocouple and devices in door at 1,9 m above floor (0,1 m below frame).

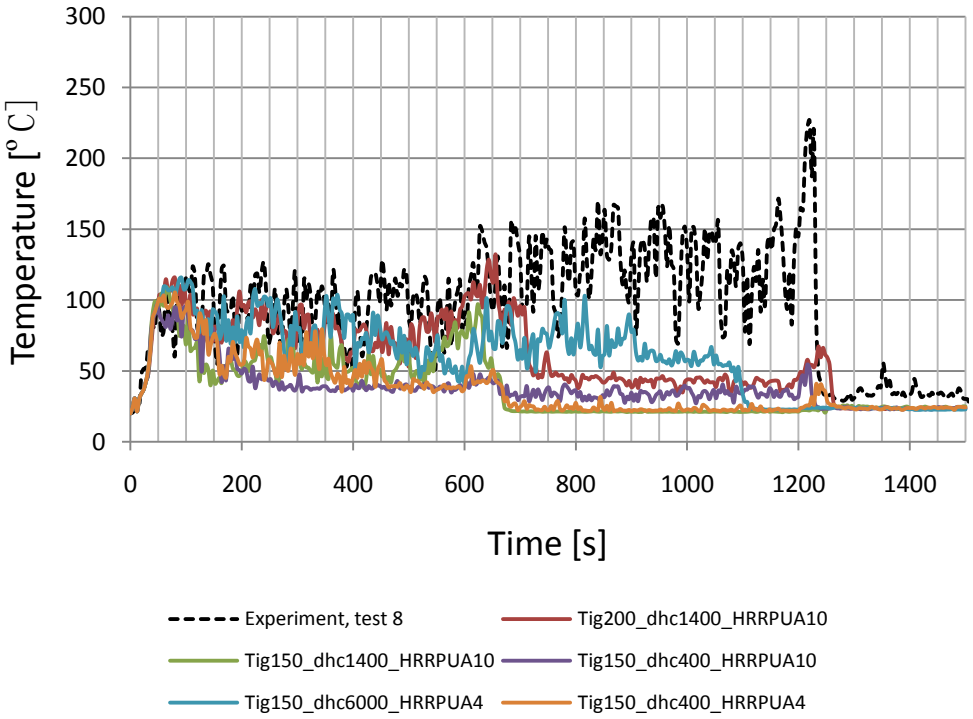

Figure 43. Model I, test 8. Thermocouple and devices in door at 1,5 m above floor (0,5 m below frame).

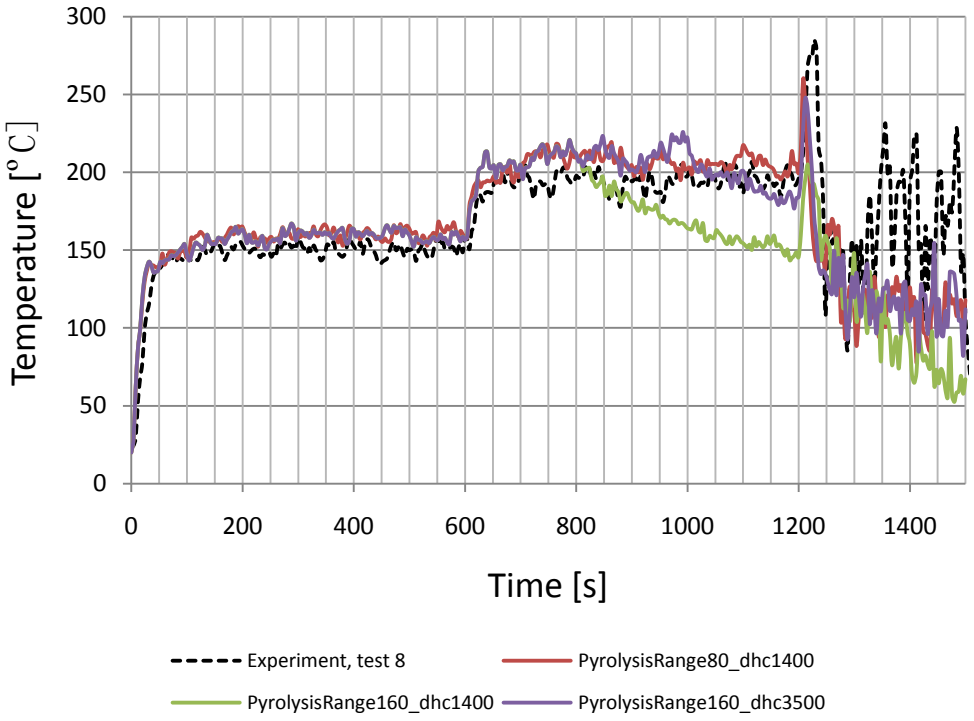

Figure 44. Model II, test 8. Thermocouple and devices in door at 1,9 m above floor (0,1 m below frame).

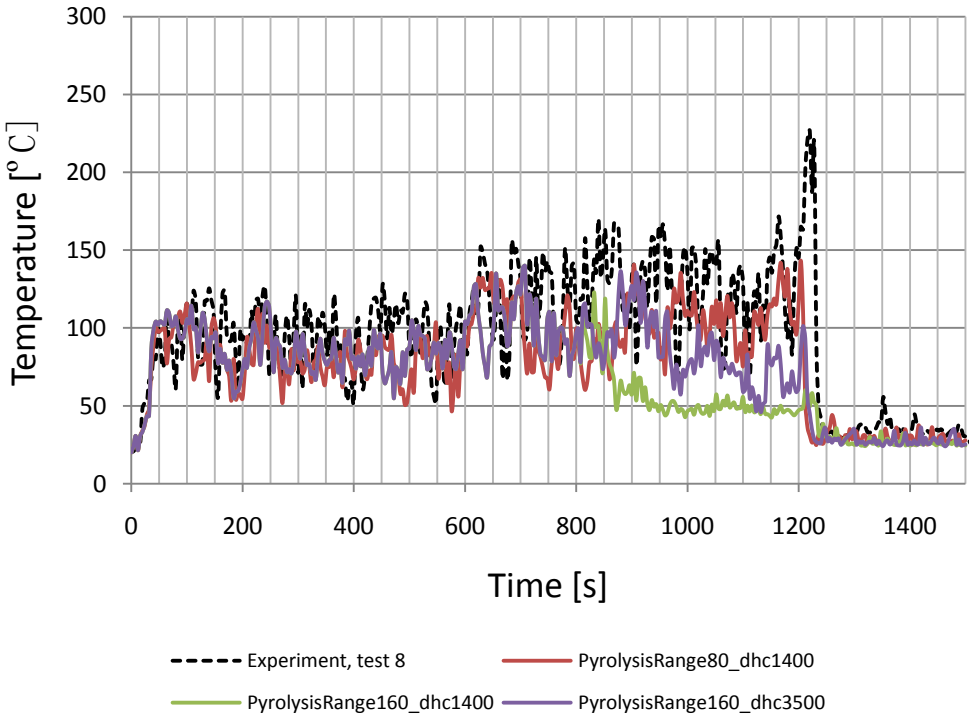

Figure 45. Model II, test 8. Thermocouple and devices in door at 1,5 m above floor (0,5 m below frame).

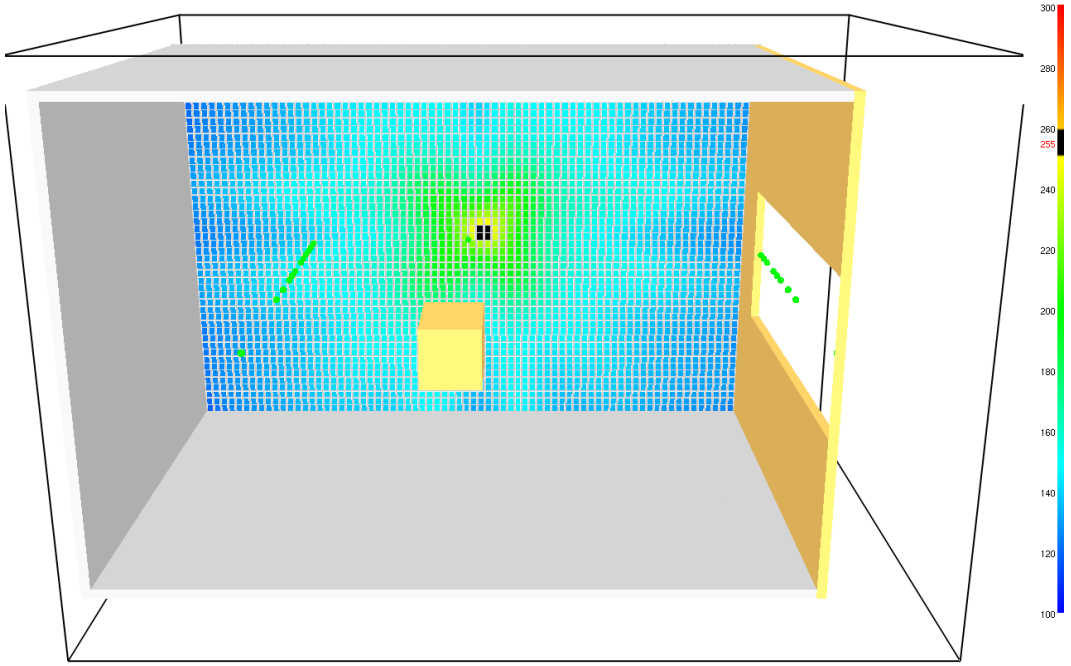

Figure 46. Test 8, model II, pyrolysis range 160, ref temp 280, ΔHc 3500, after 996 s, black indicates 255ºC.

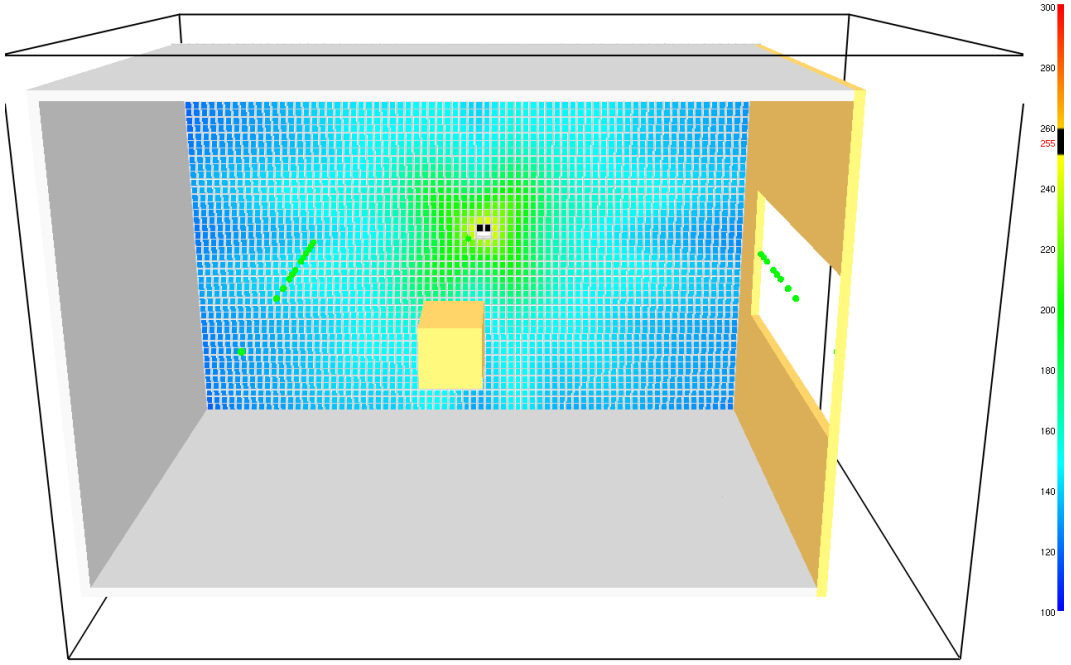

Figure 47. Same as above but, after 997,5 s, black indicates 255ºC. This shows that there can be holes before the reference temperature has been reached.

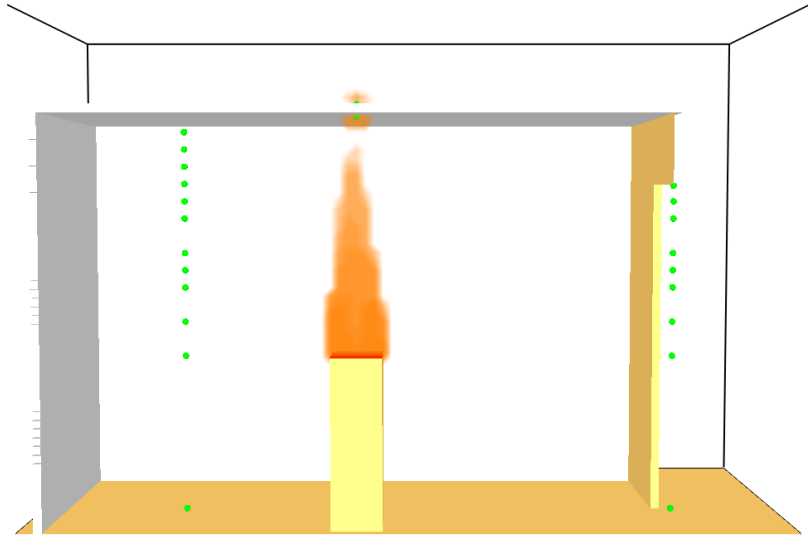

Figure 48. Test 7, model II, 5 cm grid size. After 15 s, flame > 200 kW/m³.

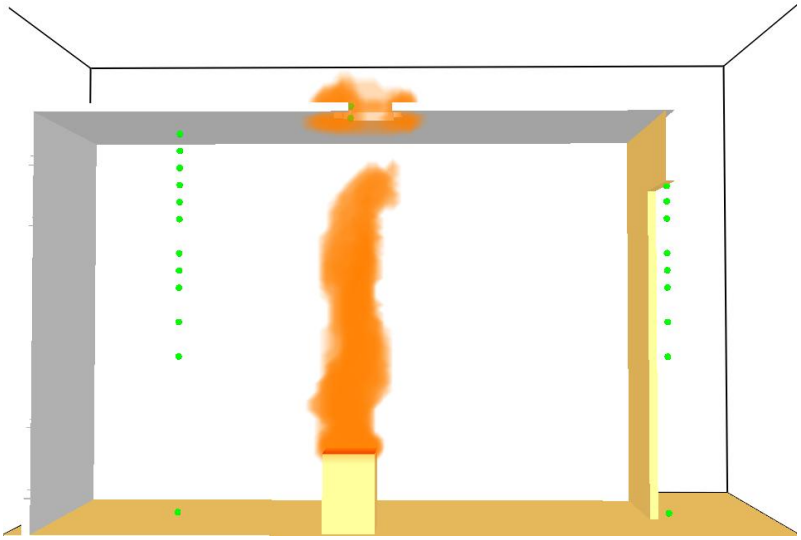

Figure 49. Test 8, model II, 5 cm grid size. After 1210,5 s, flame > 200 kW/m³.

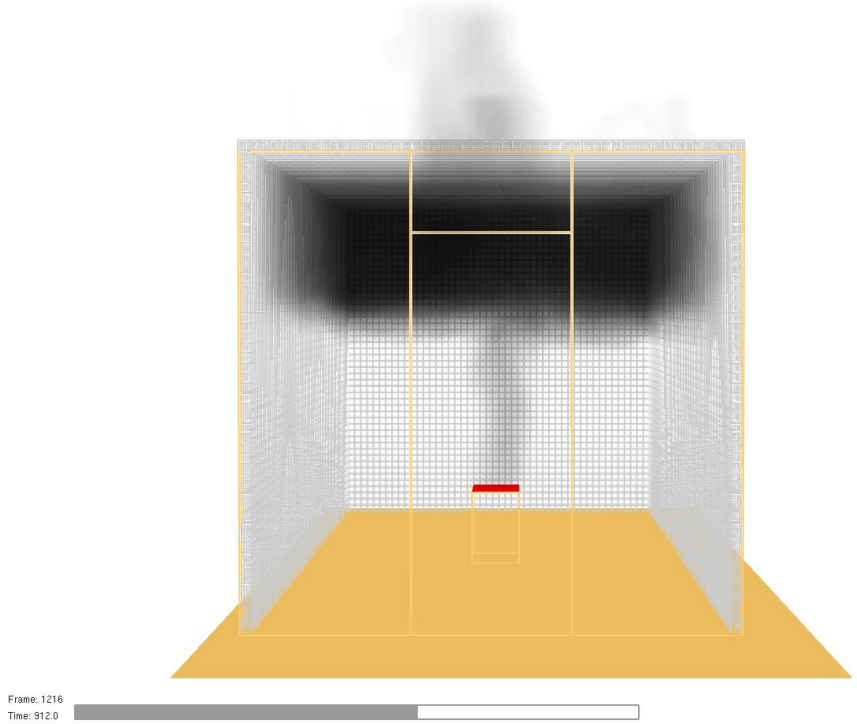

Figure 50. Test 8, model I, 5 cm grid size. After 912 s.

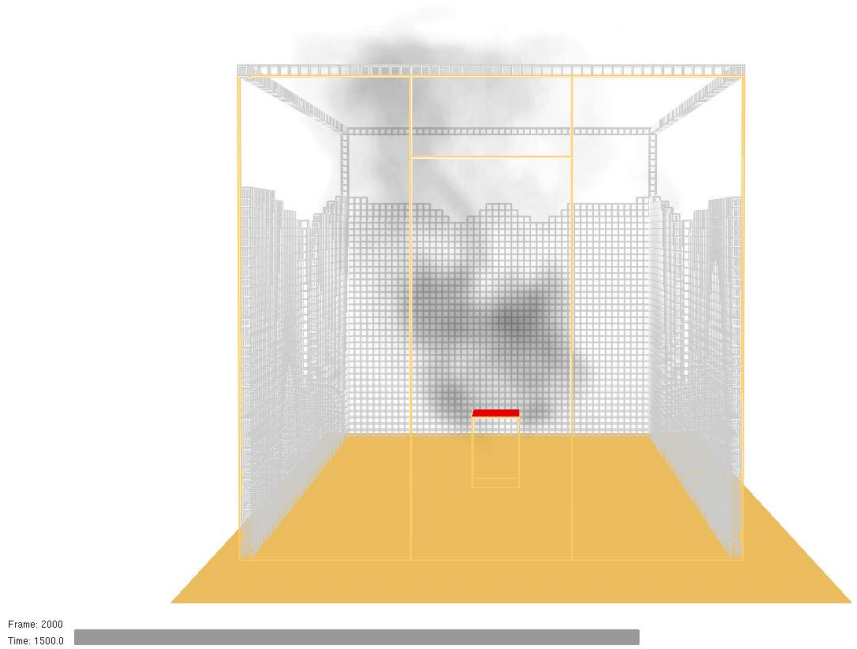

Figure 51. Test 8, model I, 5 cm grid size. After 1500 s.